Int J Earth Sci (Geol Rundsch) (2017) 106:131–155
DOI 10.1007/s00531-016-1306-3

ORIGINAL PAPER

Dynamics of prolonged salt movement in the Glückstadt Graben (NW Germany) driven by tectonic and sedimentary processes

Michael Warsitzka[1] · Jonas Kley[2] · Fabian Jähne-Klingberg[3] · Nina Kukowski[1]

Received: 9 September 2015 / Accepted: 4 February 2016 / Published online: 26 February 2016

Abstract The formation of salt structures exerted a major influence on the evolution of subsidence and sedimentation patterns in the Glückstadt Graben, which is part of the Central European Basin System and comprises a post-Permian sediment thickness of up to 11 km. Driven by regional tectonics and differential loading, large salt diapirs, salt walls and salt pillows developed. The resulting salt flow significantly influenced sediment distribution in the peripheral sinks adjacent to the salt structures and overprinted the regional subsidence patterns. In this study, we investigate the geometric and temporal evolution of salt structures and subsidence patterns in the central Glückstadt Graben. Along a key geological cross section, the post-Permian strata were sequentially decompacted and restored in order to reconstruct the subsidence history of minibasins between the salt structures. The structural restoration reveals that subsidence of peripheral sinks and salt structure growth were initiated in Early to Middle Triassic time. From the Late Triassic to the Middle Jurassic, salt movement and salt structure growth never ceased, but were faster during periods of crustal extension. Following a phase from Late Jurassic to the end of the early Late Cretaceous, in which minor salt flow occurred, salt movement was renewed, particularly in the marginal parts of the Glückstadt Graben. Subsidence rates and tectonic subsidence derived from backstripping of 1D profiles reveal that especially the Early Triassic and Middle Keuper times were periods of regional extension. Three specific types of salt structures and adjacent peripheral sinks could be identified: (1) Graben centre salt walls possessing deep secondary peripheral sinks on the sides facing away from the basin centre, (2) platform salt walls, whose main peripheral sinks switched multiple times from one side of the salt wall to the other, and (3) Graben edge pillows, which show only one peripheral sink facing the basin centre.

Keywords Salt tectonics · Glückstadt Graben · Extensional basin · Structural restoration

Introduction

In salt basins affected by tectonic stresses, horizontal strain effectively triggers the formation of salt structures. Overburden deformation is usually decoupled from the subsalt basement due to the mechanical weakness of the salt (Jackson and Vendeville 1994). Once the salt layer has been vertically displaced by basement faulting, lateral thickness changes in post-salt sediments (differential loading) can act as the main driving mechanism for further salt flow and growth of down-built salt structures (Hudec and Jackson 2007). Large accommodation space can be created due to the subsidence of characteristic minibasins in the supra-salt succession, namely primary peripheral sinks (PSP) and secondary peripheral sinks (SPS) (sensu Trusheim 1960; Hudec and Jackson 2007). The first type of minibasins is a diagnostic structure for deposition next to salt pillows or salt diapirs in an early stage of development. The second

✉ Michael Warsitzka
Michael.Warsitzka@uni-jena.de

1 Institute of Geosciences, Friedrich Schiller University Jena, Burgweg 11, 07749 Jena, Germany

2 Geoscience Centre, Structural Geology and Geodynamics, Georg-August-University Göttingen, Goldschmidtstr. 3, 37077 Göttingen, Germany

3 Federal Institute for Geosciences and Natural Resources, Stilleweg 2, 30655 Hannover, Germany

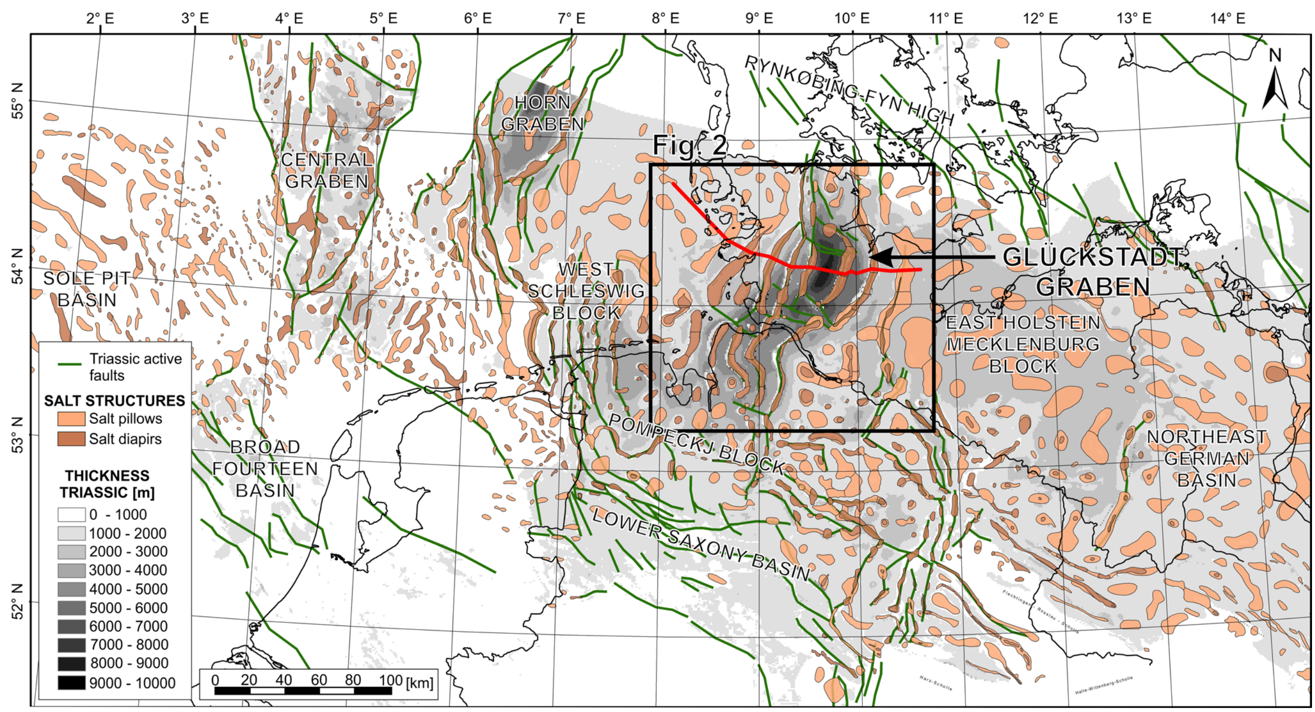

Fig. 1 Map of the Central European Basin System showing the distribution of salt structures and main faults active during Triassic. Salt structures and thickness data are modified from Doornenbal and Stevenson (2010)

type is characteristic for forming next to passively growing salt diapirs (Sørensen 1998; Hudec and Jackson 2011).

The Glückstadt Graben in north-west Germany (Fig. 1) is an excellent example for studying the evolution of salt structures and peripheral sinks in an extensional setting, since it contains some of the deepest peripheral sinks and largest salt walls found in the Central European Basin System (CEBS). First investigations of salt structure evolution in the Glückstadt Graben by Trusheim (1960) and Sannemann (1968) using seismic reflection data found that the ages of salt structures and of the sediments in the peripheral sinks progressively decreases from the basin centre towards the graben flanks. On the basis of this observation, the concept of salt stock families was proposed, which holds that daughter diapirs develop as a consequence of buoyancy forces exerted by a neighbouring mother diapir (Sannemann 1968). Later, new seismic profiles, gravity surveys and drill hole data enabled to study the deep structure and basin evolution over large areas of north-west Germany (e.g. Best et al. 1983; Bachmann and Grosse 1989; Brink et al. 1992). It became evident that regional extension was the dominant trigger for salt tectonics and diapirism (Best et al. 1983). Based on seismic lines as well as structural thickness and depth maps provided in the Tectonic Atlas of NW Germany (Baldschuhn 1996; Baldschuhn et al. 2001), regional scale 3D geological models were reconstructed (Maystrenko et al. 2005a; Hese 2012) and backstripping restorations (Frisch and Kockel 1999; Maystrenko et al. 2005b, 2006) were performed. These studies led to substantial advances in the understanding of the original distribution of the Upper Permian salt layer, the timing of tectonic phases and the salt motion. The Early and Late Triassic, the Early to Middle Jurassic and the Paleogene were identified as periods of major salt movements in the Glückstadt Graben (Frisch and Kockel 1999; Kockel 2002; Maystrenko et al. 2005b). These phases correlate with events of regional extension found in areas surrounding the Glückstadt Graben. Eventually, salt flowage resulted in the development of large salt walls and salt pillows (e.g. Maystrenko et al. 2005b). The associated expulsion of the originally up to 3000-m-thick salt succession crucially affected subsidence patterns and overprinted regional tectonic strain patterns from the Triassic to the present (Maystrenko et al. 2005b).

However, a comprehensive reconstruction of salt structure evolution in the Central Glückstadt Graben in particular for the Triassic has not yet been undertaken. In the present study, we aim to reconstruct the temporal and spatial evolution of salt structures and subsidence patterns in the Glückstadt Graben by means of sequential decompaction and restoration of the peripheral sinks. Furthermore, we provide subsidence curves and subsidence rates of the sedimentary succession in the peripheral sinks. Although salt flowage is usually three dimensional (Rowan and Ratliff 2012), up to 100-km-long salt walls and elongated

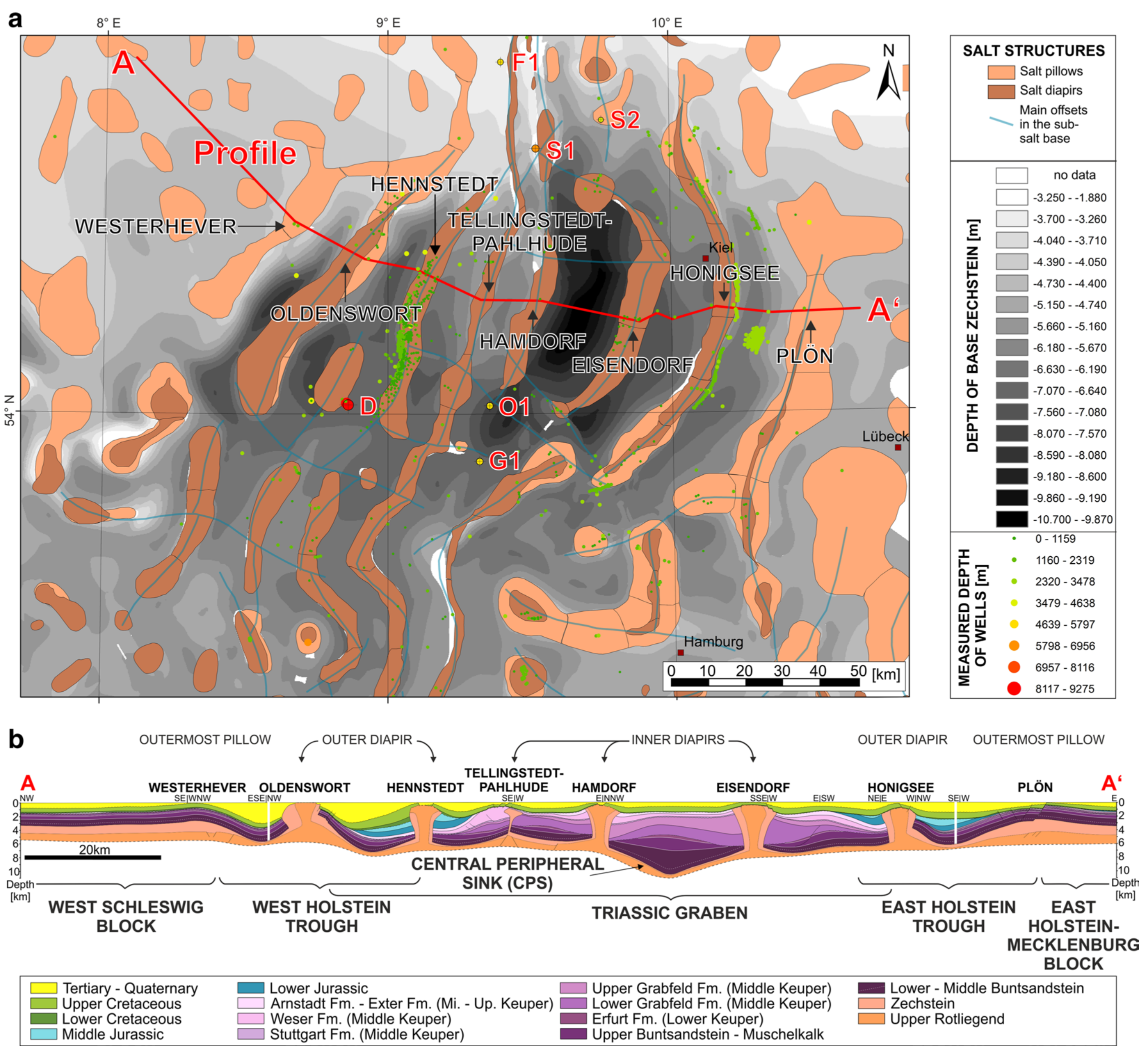

Fig. 2 **a** Map of the Glückstadt Graben area displaying the base of Zechstein (Late Permian), outlines of present-day salt structures (after Reinhold et al. 2008), locations of wells with maximum depths colour-coded and the trace of the cross section (*red*). Deep wells are labelled: D Dieksand, F1 Flensburg Z1, G1 Glückstadt T1, O1 Oldenbuettel T1, S1 Schleswig Z1, S2 Steinfeld Z1. Note that due to horizontal deviation of the well path, the measured depth of the wells is usually higher than the true vertical depth. **b** Cross section of the Central Glückstadt Graben displaying salt walls and sedimentary patterns of the post-Permian strata (modified from Baldschuhn 1996). The depth of the Top Lower Buntsandstein (*white dashed line*) was inferred from regional thickness maps (Doornenbal and Stevenson 2010)

depocentres striking mostly parallel to the graben axis of the Glückstadt Graben suggest that salt flowed mainly perpendicular to the graben axis. Therefore, this study focuses on a representative geological cross section that is based on a seismic interpretation (Baldschuhn 1996) and crosses the entire central Glückstadt Graben (Fig. 2).

Geological and structural setting

The NNE-SSW to NE-SW striking Glückstadt Graben is part of an assembly of scattered Permo-Triassic extensional basins within the larger Central European Basin System (CEBS) (Maystrenko et al. 2006; Littke et al. 2008; Scheck-Wenderoth et al. 2008a) (Fig. 1). The Glückstadt Graben is framed by the Rynkøbing-Fyn High to the north and the Pompeckj Block to the south. To the east and west, the Glückstadt Graben is surrounded by platforms of almost undeformed sediments (West Schleswig Block, East Holstein-Mecklenburg Block).

In the basin centre, numerous more than 6000-m-high salt walls coincide with offsets in the sub-salt basement (Fig. 2). The mobile layer building the salt structures contains Upper Rotliegend and Zechstein (Upper Permian) evaporites. Three-dimensional forward modelling predicts an original salt layer (Upper Rotliegend and Zechstein) thickness of as much as 3000 m in the basin centre, approximately 1500 m on the eastern flank and 1700 m on the western flank of the graben (Maystrenko et al. 2005a). Information on the nature and the configuration of the subsalt basement in the basin centre is sparse due to the lack of deep boreholes and because seismic imaging is heavily impaired by the strong attenuation of seismic energy at the boundaries of the salt layer (Baykulov et al. 2009; Maystrenko et al. 2005b).

The Glückstadt Graben contains the thickest Meso-Cenozoic succession of the entire CEBS (~11 km). Triassic strata exhibit their maximum thickness in a ~20-km-wide trough in the central part of the Glückstadt Graben, which extends roughly 100 km in north–south direction. In particular, Middle to Upper Keuper (Upper Triassic) sediments fill up to 6000-m-deep asymmetric peripheral sinks adjacent to the inner salt walls (Tellingstedt-Pahlhude, Hamdorf and Eisendorf). According to Maystrenko et al. (2005a), the region of increased Triassic thickness is here referred to as the Triassic Graben (Fig. 2b). Lower to Middle Jurassic sediments are only preserved in secondary peripheral sinks of the outer, Hennstedt and Honigsee salt walls. Lower to Upper Cretaceous strata cover the innermost salt walls and are only slightly thickened in the peripheral sinks of the Hennstedt and Honigsee structures. Cenozoic sediments display again increased thicknesses adjacent to all salt walls in two marginal troughs, the West Holstein Trough and the East Holstein Trough (Maystrenko et al. 2005a). In the outer part of the basin, the Glückstadt Graben is bounded by undeformed areas of the West Schleswig Block and the East Holstein-Mecklenburg Block. The basic structural pattern of main depocentres and salt walls continues northward of the cross section for roughly 50 km and southward for roughly 100 km (Fig. 2a) (Baldschuhn et al. 2001; Maystrenko et al. 2005a).

Tectonic evolution

The early tectonic history of the region of the Glückstadt Graben supposedly started with transtensional tectonics during the Late Carboniferous to Early Permian, which was associated with faulting and igneous activity (Ziegler 1982, 1990; Gast and Gundlach 2006; Kley et al. 2008). The Permian transtension was followed by a long-lasting period of thermal subsidence in the entire Permian Basin from the Late Permian to the beginning of the Early Triassic (e.g. Bachmann and Grosse 1989; Van Wees et al. 2000; Littke et al. 2008). During the Triassic, thermal subsidence was interrupted by numerous episodes of regional extension indicated by variations in sedimentary onlap patterns (e.g. Maystrenko et al. 2006) and locally increased subsidence rates (e.g. Littke et al. 2008; Rodon and Littke 2005). This extension led to segmentation of the larger Southern Permian Basin (Doornenbal and Stevenson 2010) into separated grabens or troughs, e.g. the Glückstadt Graben, the Horn Graben or the Central Graben (Kley et al. 2008; Van Wees et al. 2000). Early phases of post-Permian extension in the Glückstadt Graben are postulated for the Early Triassic (Middle Buntsandstein time: mainly Detfurth and Hardegsen Formations) and for the Middle Triassic (Upper Buntsandstein–Middle Muschelkalk) (Röhling and Gast 1991; Brink et al. 1992; Kockel 2002). During these events, a relatively narrow graben formed in the centre of the Glückstadt Graben (Brink et al. 1992). In Late Triassic times (Grabfeld Formation and Weser Formation time), E-W-directed extension occurred in the area of the Glückstadt Graben ("Early Kimmerian phase") (Frisch and Kockel 1999; Jaritz 1987; Kockel 2002; Maystrenko et al. 2006; Ziegler 1982). This caused a widening of the graben and intense salt movements including diapirism (Brink et al. 1992; Maystrenko et al. 2005a). In Middle to Late Jurassic times, regional NE-SW extension prevailed ("Middle Cimmerian phase") in some parts of the CEBS (Kockel 2002; Kley et al. 2008). This event probably affected the marginal parts of the Glückstadt Graben (Maystrenko et al. 2005a), but far less than the neighbouring areas, in particular Lower Saxony Basin to the south. A major interruption of sedimentation and regional erosion in the area around the Glückstadt Graben can be recognised from the Kimmeridgian to the Valanginian (Late Jurassic–Early Cretaceous (Maystrenko et al. 2005a). The depth of erosion is estimated to be roughly 800 m in the central area of the Glückstadt Graben (Maystrenko et al. 2005a; Littke et al. 2008). The Late Cretaceous is a phase of enhanced subsidence in the Glückstadt Graben. From Coniacian to Campanian, a NW-SE-directed shortening regime prevailed in Central Europe (Kley et al. 2008; Ziegler 1990), which significantly affected regions adjacent to the Glückstadt Graben (e.g. Lower Saxony Basin). In the Glückstadt Graben, roofs of the diapirs were slightly uplifted at the end of Cretaceous, which is probably a result of this regional compression (Maystrenko et al. 2006). During Eocene to Miocene time, ESE-WNW to E-W extension and contemporary NE-SW compression prevailed in Central Europe (Kley et al. 2008; Scheck-Wenderoth et al. 2008b). In this period, subsidence rates in the West Holstein Trough and in the East Holstein Trough attained its maximum (Maystrenko et al. 2005a).

Sedimentary history

The lack of deep wells prevents exact identification of sedimentary facies in the centre of the Glückstadt Graben. However, information about the stratigraphic succession in the central Glückstadt Graben was obtained from wells located on structural highs in the Glückstadt Graben (see Fig. 2a for location) and correlated with the centre of the

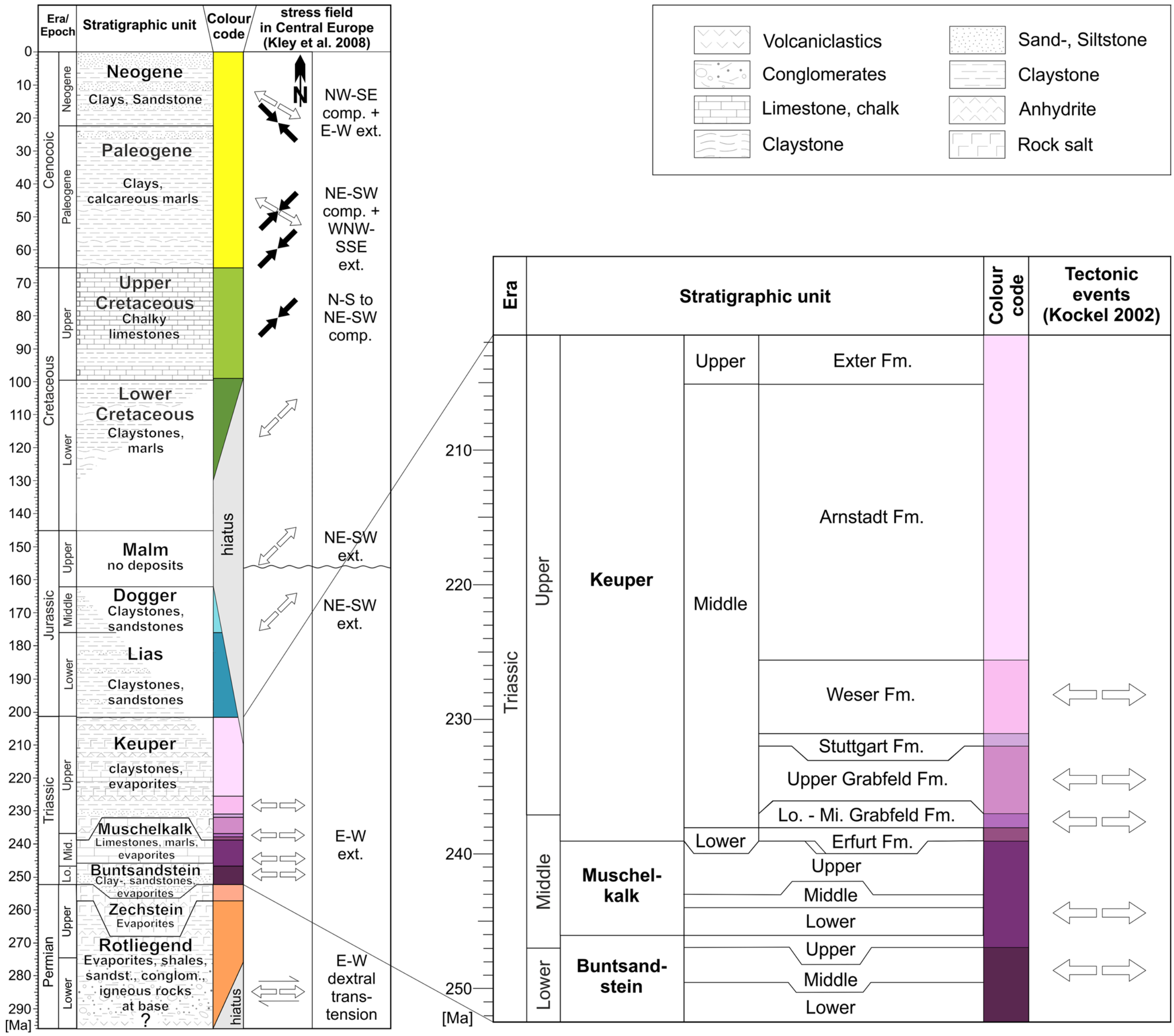

Fig. 3 Stratigraphy of the Glückstadt Graben (modified from Maystrenko et al. 2005a; Rodon and Littke 2005; Barnasch 2010). Colour coding of stratigraphic units as in the geological cross section

basin (Maystrenko et al. 2005b). The stratigraphic succession in the area of the Glückstadt Graben can be divided into three main parts (Maystrenko et al. 2005b): (1) the basement beneath the main salt layer consisting of clastic sediments, which are likely of Late Devonian to Early Permian age, (2) Lower to Upper Permian evaporites building the salt structures and (3) the Mesozoic to Cenozoic post-salt succession (Fig. 3).

The basement beneath the Permian salt is characterised by conglomerates and volcaniclastics, which grade upwards into clays and evaporites (Maystrenko et al. 2005b). The Permian Rotliegend evaporite succession consists mostly of rock salt (~55 % of the Rotliegend succession) with intercalated carbonates and clastics deposited in sabkha and desert lake environments (Maystrenko et al. 2005a). The Zechstein consists of seven more or less complete evaporation cycles (dominantly rock salt, carbonates, anhydrites and potassium salts) deposited under marine conditions (Stollhofen et al. 2008). The sedimentary succession of the Triassic starts with continental deposits of the Lower to Middle Buntsandstein (Lower Triassic) mainly consisting of fluvio-lacustrine siliciclastics and minor evaporites (Lepper et al. 2013). Marine conditions from Late Buntsandstein until the end of Muschelkalk (Middle Triassic) time lead to the sedimentation of shallow marine limestones and marlstones with significant intercalations of evaporites in the Upper Buntsandstein (Roet) and the Middle Muschelkalk (Stollhofen et al. 2008). During Keuper time (Late

Middle Triassic–Late Triassic), depositional environments in the CEBS changed back to continental facies (Barnasch 2010). The Erfurt Fm. (Lower Keuper) mainly contains siliciclastics deposited in a continental and partly marine environment (Beutler 2005; Stollhofen et al. 2008). The Middle Keuper Grabfeld and Weser Fms. are dominated by sabkha and playa facies represented by claystones and siltstones and widespread intercalations of evaporites (mainly anhydrites and rock salt). Both formations are separated by the Stuttgart Fm. consisting of fluvio-deltaic sandstones (Stollhofen et al. 2008). The Arnstadt Fm. (Middle Keuper) contains mudstones of playa lake origin. The Exter Fm. (Upper Keuper) is characterised by a transition of continental environments to marine conditions dominated during Jurassic (Stollhofen et al. 2008). Sediments of Early to Middle Jurassic age are composed of shallow marine carbonates and marine clastics (Stollhofen et al. 2008). After a major hiatus from Late Jurassic time to the beginning of the Early Cretaceous, fluvio-deltaic claystones and subordinate sandstones were deposited unconformably over Triassic and Jurassic strata (Maystrenko et al. 2005a). The global eustatic sea level highstand led to deposition of chalky limestones during the Late Cretaceous. An additional erosional unconformity separates Mesozoic and Cenozoic sediments. Since the Early Tertiary, fluvial and lacustrine clastics prevailed (Stollhofen et al. 2008).

Data base and method

The available data consist of a geological cross section (Fig. 2b) provided in the Geotectonic Atlas of Northern Germany (GTA) (Baldschuhn 1996; Baldschuhn et al. 2001). The cross section is based on interpreted 2D seismic data. Depth migration of the interpreted seismic line is based on Jaritz et al. (1991). In order to show the structures on the platforms bounding the Glückstadt Graben, we used two additional cross sections from Baldschuhn et al. (2001), which have been attached to the east and west of the original cross section (Baldschuhn et al. 2001). This cross section is similar to other seismic sections trending parallel to it (Baldschuhn et al. 2001; Baykulov et al. 2009; Maystrenko et al. 2005a) and is therefore taken to be representative of the general structural framework of the Glückstadt Graben. The post-Permian sedimentary succession is subdivided into 13 units (Table 1). The geological cross sections of the Geotectonic Atlas of Northern Germany are based on depth-migrated seismic interpretations, which were correlated with borehole data (Baldschuhn et al. 2001; Hese 2012). Nevertheless, there are ongoing debates concerning the accuracy of the interpretation in particular for the base of the Lower Triassic, the base of the Permian salt layer and the pre-Permian layers (e.g. Bayer et al. 2003; Maystrenko et al. 2005b).

Decompaction and restoration

Compaction and subsidence were sequentially restored using simple shear along vertical planes (Bishop et al. 1995; Buchanan et al. 1996; Rowan 1993). The work procedure included decompaction and vertical simple shear restoration of all post-Permian layers employing the 2DMOVE™ software package (Midland Valley) to obtain the sequential evolution of sediment accumulation for each unit. As is common usage, the decompaction tool available in 2DMOVE™ assumes that porosity is mostly lost due to mechanical compaction, while chemical compaction is not included. Thus, porosity gradually decreases according to an equation first presented by Athy (1930):

$$\phi(z) = \phi_0 e^{-cz} \quad (1)$$

where Φ is the porosity, Φ_0 the initial porosity, c the compaction factor and z the burial depth. Lithological and petrophysical data (density, initial porosity) used for the decompaction calculation (Table 1) were taken from published data from the Glückstadt T1 (Rodon and Littke 2005), Schleswig Z1, Flensburg Z1, and Oldenbuettel T1 wells (Schöner 2006) (see Fig. 2 for location) as well as from stratigraphic studies (Barnasch 2010; Lepper et al. 2013). Using this information, the average lithological composition was estimated for each stratigraphic unit considered here (Table 1). For the compaction factor c, default values implemented in the MOVE™ software package (Midland Valley), Yegorova et al. (2008) and Allen and Allen (2013) were used. Initial porosities and porosity–depth coefficients applied here (see used values in Table 1) represent average values with regard to the lithological composition. A reduced depth coefficient of 0.1 was assigned for the Lower Triassic sandstones instead of using a standard porosity–depth factor $c = 0.27$ for sandstone. It has been shown that sandstones of the Lower Triassic Buntsandstein in the North German Basin and the Netherlands possess high porosities (25–35 %, including cements) due to early cementation even at greater depth (1500–4000 m) (e.g. Purvis and Okkerman 1996; Wolfgramm et al. 2008). However, Lower Triassic clays were assumed to compact with a standard coefficient of $c = 0.51$, which results in an average compaction coefficient of $c = 0.305$ for the Lower to Middle Buntsandstein unit (Table 1).

In order to estimate errors on decompacted layer thicknesses of all units, a sensitivity study was carried out applying maximum and minimum values for initial porosity and compaction coefficients (Table 1).

Table 1 Lithologies and petrophysical parameters used for decompaction procedure and sensitivity analysis

Unit/ formation	Age of top (Myr)	Lithology	% Sandstone	% Claystone	% Chalk	% Limestone	% Evaporites	c (min) [km^{-1}]	c (max) [km^{-1}]	c (used) [km^{-1}]	ϕ_0 (min)	ϕ_0 (max)	ϕ_0 (used)	ρ_G[$kg\ m^{-3}$]
Tertiary + Quaternary	0	SHALE, SHALEsand, SANDshale[1, 2]	0.4	0.6	0	0	0	0.27	0.51	0.414	0.48	0.57	0.558	2680
Upper Cretaceous	65.5	CHALK, Limeshaly[1, 2]	0	0.1	0.7	0.2	0	0.68	0.71	0.69	0.57	0.65	0.568	2709
Lower Cretaceous	99.5	SHALEcarb[1, 2]	0	0.8	0.2	0	0	0.4	0.71	0.55	0.52	0.52	0.65	2702
Upper Jurassic	145.5	No sediments	–	–	–	–	–	–	–	–	–	–	–	–
Middle Jurassic	162	SHALEsand[1, 2]	0.3	0.7	0	0	0	0.33	0.51	0.438	0.63	0.63	0.581	2685
Lower Jurassic	176	SHALE, SHALEsand, SHALEcalcsand[1, 2]	0.1	0.8	0.1	0	0	0.33	0.71	0.506	0.55	0.57	0.627	2696
Arnstadt–Exter Fm. (Middle–Upper Keuper)	201.5	SHALEcarb, SHALEevap, SHALEsand[1, 2, 4]	0.1	0.5	0.3	0	0.1	0.39	0.71	0.478	0.48	0.62	0.563	2688
Weser Fm. Middle Keuper	226	SHALEcarb, SALT[1, 2, 4]	0	0.4	0.1	0	0.5	0	0.51	0.275	0.52	0.62	0.33	2651
Stuttgart Fm. (Middle Keuper)	231	SAND&SHALE, SHALEsand[1, 2, 4]	0.2	0.8	0	0	0	0.27	0.51	0.428	0.49	0.52	0.604	2690
Upper Grabfeld Fm. (Middle Keuper)	234	SHALEcarb, SHALEevap, SALT[1, 2, 4]	0	0.6	0	0	0.4	0	0.51	0.306	0.47	0.62	0.394	2660
Lower–Middle Grabfeld Fm. (Middle Keuper)	237	SHALEcarb, SHALEevap, SALT[1,2, 4]	0	0.6	0	0	0.4	0	0.51	0.306	0.47	0.62	0.394	2660
Erfurt Fm. (Lower Keuper)	238	SHALEcarb, SHALE[1,2, 4]	0	0.8	0.2	0	0	0.51	0.71	0.55	0.62	0.65	0.65	2702

Table 1 continued

Unit/ formation	Age of top (Myr)	Lithology	% Sandstone	% Claystone	% Chalk	% Limestone	% Evaporites	c (min) [km^{-1}]	c (max) [km^{-1}]	c (used) [km^{-1}]	ϕ_0 (min)	ϕ_0 (max)	ϕ_0 (used)	ρ_G[kg m^{-3}]
Upper Buntsandstein–Muschelkalk	238.8	LIME, SHALEevap, MARLcarb[1,2]	0	0.3	0.1	0.3	0.3	0	0.71	0.344	0.39	0.47	0.335	2674
Lower–Middle Buntsandstein	247.1	SAND&SHALE, SHALEsand, SHALE-calcsand[1,2,3]	0.4	0.6	0	0	0	0.27	0.51	0.346	0.52	0.57	0.558	2680
Zechstein	252.7	EVAPORITES[1,2]	0	0	0	0	1	–	–	–	0	0	0	2685
Upper Rotliegend	260.5	EVAPshaly, SHALEsilt[1,2]	0	0.5	0	0	0.5	–	–	–	–	–	–	2600

Capital letters in the description of the lithologies denote the main lithologic component. Chronostratigraphic ages of layer boundaries came from Kozur and Bachmann (2008) and Littke et al. (2008). Default values for *c* according to each lithology came from Schöner (2006). ρ_G is the average grain density. References for lithology: (1) Rodon and Littke (2005), (2) Schöner (2006), (3) Barnasch (2010), (4) Lepper et al. (2013). Reference for ϕ_0: Schöner (2006). Default values for c are (Sclater and Christie 1980), 2DMOVE™ software package): shale: 0.51, sand: 0.27, chalk: 0.71, limestone: 0.4, evaporites: 0.0

In the reconstruction procedure presented here, the load effect of the uppermost layer is removed, whereupon all underlying layers decompact. All decompacted horizons are then restored applying vertical shear restoration. The top of the uppermost layer is made horizontal, and all deeper layers are passively uplifted with equal vertical displacement vectors. The vertical shear restoration preserves the thickness of each layer, but distorts horizon lengths. We assume that three-dimensional salt flow is balanced by vertical movement of the post-salt peripheral sinks. Therefore, two-dimensional restoration of the subsidence of post-salt layers can be applied, if the cross section is chosen to strike perpendicular to main trend of the elongated salt structures and the tectonic fault pattern in the sub-salt basement (Hossack 1995).

The structural restoration was limited to the post-salt layers, since neither the salt layer nor the sub-salt basement could be restored directly. This is because the present-day geometry of the top basement is difficult to identify in seismic data (see model limitation). However, for subsidence curves and interpretive sketches, the configuration of the basement was drawn by assuming a maximum original salt layer (Zechstein and Upper Rotliegend) thickness of 1500 m above the eastern graben flank and 3000 m in the basin centre (Maystrenko et al. 2005a) and by adopting the basement faults shown on the structural map of Northern Germany provided by the GTA (Baldschuhn et al. 2001). For the sake of simplicity, both Permian evaporite successions (Upper Rotliegend and Zechstein) are considered as a single mobile layer named "salt layer" throughout this paper. The basement beneath the salt layer thus corresponds to the base of the salt-rich Rotliegend. Furthermore, the term "pre-kinematic" is used for sediments deposited before salt structure growth, "syn-pillow" for sediments accumulated in primary peripheral sinks (sensu Hudec and Jackson 2011) during the salt pillow stage and "syn-diapiric" for sediments accumulated in secondary peripheral sinks (sensu Hudec and Jackson 2011) attributable to a specific salt diapir. Furthermore, salt structures in the transitional stage from pillow to diapir are called "immature", salt structures in a downbuilding stage are called "mature", and diapirs which ceased to grow are named "dormant diapirs". The side of a salt structure is called "inner side" if it faces the centre of the graben and "outer side" if it faces the graben flanks.

Subsidence curves, subsidence rates and salt structure growth

Decompacted layer thicknesses were measured across 102 1D profiles along the restored cross section for each time step. This enables us to quantify (1) magnitudes of salt structure growth, (2) the total subsidence, and (3) subsidence rates averaged for each time interval considered here.

1. The amount of growth of each salt structure was determined from the thickness changes in the neighbouring peripheral sinks assuming that growth can be calculated by the relative difference between the thickness of neighbouring sediments and the crest of the salt structure. Furthermore, we assumed that salt structures pass through the pillow stage as long as they are surrounded by primary peripheral sinks and that they enter the diapiric stage as soon as they are encompassed by secondary peripheral sinks. During the pillow stage, amounts of growth h_P are defined as half the maximum thickness of the adjacent primary peripheral sinks minus the thickness above the pillow crest (Fig. 4) (Seni and Jackson 1983). For the diapir stage, the amount of growth h_D equals the average maximum thickness of the secondary peripheral sink on both sides of the diapir (Fig. 4). Values determined by this method have to be considered as first-order estimates. This is because, near-surface salt dissolution and erosion of sediments from the peripheral sinks cannot be quantified, but may enhance or reduce the actual amount of growth (see model limitations).
2. Following the backstripping procedure of Allen and Allen (2013), 1D tectonic subsidence curves were calculated from total subsidence. The tectonic subsidence S_{tec}—this contains fault-induced subsidence, thermal subsidence and subsidence induced by salt expulsion—was calculated by subtracting the Airy isostatic subsidence induced by the sediment load from the total subsidence and by correcting it for paleo-water depth S_{PW} and eustatic sea level change ΔS_{SL} (Allen and Allen 2013):

$$S_{tec} = H\left(\frac{\rho_M - \overline{\rho_S}}{\rho_M - \rho_W}\right) - \Delta S_{SL}\left(\frac{\rho_W}{\rho_M - \rho_W}\right) + (S_{PW} - \Delta S_{SL}) \quad (2)$$

Here, H is the total decompacted sedimentary thickness, ρ_M the density of the mantle (3300 kg/m^3), ρ_W the density of sea water (1050 kg/m^3), and $\overline{\rho_S}$ the average bulk density of the entire sedimentary column. Information about paleo-water depths came from well data (Schöner 2006 and references therein), and values of the eustatic sea level change were taken from Haq et al. (1987).

Since the basement of the salt layer was excluded from the restoration procedure, we refrained from reconstructing the amount of basement extension and the exact backstripping of the basement of the salt layer. However, we attempted to distinguish the effect of subsidence induced by salt expulsion S_{sa} from tectonic subsidence. We assumed a specific initial thickness of the Upper Permian salt layer (as explained above) at the end of Permian. This thickness decreases beneath peripheral sinks and increases in regions of salt structure uplift (e.g. growing salt pillows) through time. Hence, we defined an amount of thickness change in the salt layer for each time step, which was either added to or subtracted from the original salt layer thickness, respectively. The magnitude of these thickness changes in each time interval was estimated by the depth of the crestal erosion or the depth of the peripheral sink in relation to the regional thickness of each layer. Based on estimations of subsidence induced by salt flowage, the Upper Permian salt layer can be added to the total subsidence of the base Buntsandstein and, therefore, incorporated into the backstripping procedure (Eq. 2). Eventually, that gives the tectonic subsidence for the base of the salt layer.
3. Subsidence rates were calculated by dividing the incremental total subsidence of the base of the Buntsandstein by duration of the considered time interval. This calculation provides subsidence rates without including subsidence due to sediment compaction. Furthermore, it underestimates subsidence rates in periods of low temporal resolution of the layering, e.g. the Cretaceous or the Tertiary.

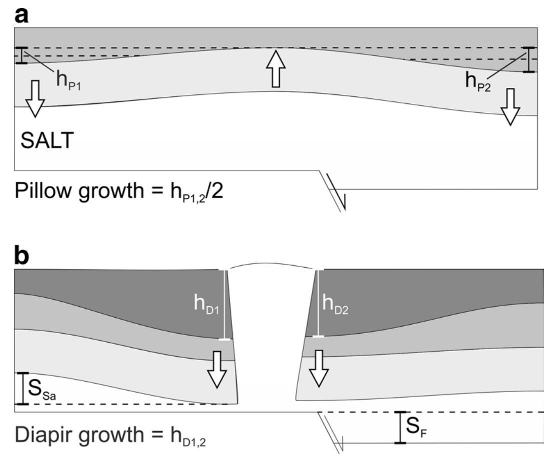

Fig. 4 Sketch showing the method for calculating net growth of a salt structure. **a** Growth of a salt pillow equals half of the layer thinning above the pillow crest assuming that layer thinning is syn-depositional. The other half of $h_{P1/2}$ is accounted for the subsidence of the peripheral sink. **b** Growth of a diapir is calculated by the depth of the surrounding secondary peripheral sink assuming that the top of the diapir remains at or close to the surface. Additionally, the amounts of fault-induced subsidence S_F and subsidence induced by salt expulsion S_{Sa} are indicated

Results

Evolution obtained from 2D-retro deformation

Figure 5 shows the sequentially restored cross sections in a chronological sequence. This illustration summarises the evolution of peripheral sinks in the Glückstadt Graben.

First phase: Buntsandstein to Early Keuper time

The post-Permian evolution of the Glückstadt Graben started with the formation of a deep approximately 15-km-wide basin-centred synclinal depocentre, here referred to as central peripheral sink (CPS) (Fig. 5a). In the CPS, the decompacted thickness of Lower to Middle Buntsandstein layers reaches 4500 m and decreases to roughly 1500 adjacent to the innermost salt structures. The thickness of the Lower–Middle Buntsandstein averages 1000–1200 m above the West Schleswig Block. In the western part of the Glückstadt Graben, the thickness of the Lower to Middle Buntsandstein varies adjacent to some salt structures (Tellingstedt-Pahlhude, Hennstedt). These thickness variations indicate development of normal faults and local, 5- to 10-km-wide uplifts. Above the East Holstein-Mecklenburg Block, the Lower to Middle Buntsandstein is nearly isopachous. Here, differences in thickness probably began to develop adjacent to the Honigsee salt diapir first in the period from Late Buntsandstein to Muschelkalk time.

Upper Buntsandstein to Lower Keuper strata taper towards the boundaries of the salt walls and are thickest in the centres between the salt structures. This led to the formation of symmetric bowl-shaped primary peripheral sinks (PPS) (Fig. 5b). Furthermore, erosional unconformities of Buntsandstein to Lower Keuper units are spatially associated with salt structures (Fig. 2). This indicates that part of the thickness decrease close to the salt structures is due to post-depositional erosion on top of rising salt structures. The pattern of increased subsidence in the centres of the PPSs continued until the end of Early Keuper time without significant lateral migration of the main depocentres.

Second phase: Middle Keuper to Middle Jurassic time

With the beginning of the Grabfeld Fm. (Middle Keuper) time, increased layer thickness is found over an approximately 70-km-wide region (Triassic Graben) (Fig. 5c, d). In this region, thicknesses of Middle to Upper Keuper strata range from 1000 to 6000 m. The depocentres in the peripheral sinks moved from the centres of the PPSs towards their flanks. This shift caused the formation of asymmetric wedge-like deposits (secondary peripheral sinks) adjacent to the salt wall boundaries and of double-wedge-like turtle-back structures (sensu Hudec and Jackson 2011), e.g. between the innermost salt structures.

Fig. 5 2D restoration of the supra-salt (post-Permian) strata. **a**, **b** ▶ Phase 1: The central peripheral sink subsides. Additional thickness variations occur above the graben flanks. **c**, **f** Phase 2: Adjacent to the innermost salt structures deep secondary peripheral sinks develop. Until the Middle Jurassic, locations of main depocentres migrate towards the graben flanks. **g**, **h** Phase 3: Most salt structures become buried by Lower Cretaceous sediments and are partly reactivated during the Tertiary. The outermost salt structures are most active during this phase. The geological cross section (**h**) was modified from Baldschuhn (1996). Note that horizontal strain (mostly extensional) is not considered. Locations of the present-day diapirs are covered with transparent areas in the reconstructed cross section, which does not imply whether each salt structure is in a diapir stage or still covered by overburden in the specific period. The depth of the Top Lower Buntsandstein (white dashed line) was inferred from regional thickness maps (Doornenbal and Stevenson 2010). Black triangles denote locations of main depocentres. CPS—Central peripheral sink, PPS—Primary peripheral sink, SPS—Secondary peripheral sink

During deposition of the Lower to Middle Grabfeld Fm., SPSs first developed close to the salt structures of Tellingstedt–Pahlhude, Hamdorf and Eisendorf. During this short period (~1 Myr), subsidence peaked at ~4500 m in the eastern SPS of the Eisendorf salt wall. The main depocentres (areas of strongest subsidence) are located adjacent to the innermost salt structures, but opposite the CPS. During Upper Grabfeld Fm. time, the main depocentres switched back to the inner side of the innermost diapirs (Fig. 5d). In this period, maximum decompacted layer thicknesses ranged from 2500 to 3500 m. No significant SPSs formed adjacent to the outer salt structures of Oldenswort, Hennstedt and Honigsee. However, layer thinning and erosional unconformities close to these salt structures (Fig. 2) indicate continued uplift since phase 1.

During deposition of the Stuttgart and Weser Fms. (Late Middle Keuper time), the deepest SPS developed next to the salt structure of Tellingstedt–Pahlhude, where these formations are as thick as 2200 m (Fig. 5e). During Arnstadt and Exter Fm. time, SPSs occurred next to the outer salt structures Hennstedt and Honigsee. Subsidence close to the innermost diapirs (Eisendorf, Hamdorf) continued. However, thicknesses of the Arnstadt and Exter Fms. next to these salt structures are smaller than those of the Grabfeld Fm.

In the latest stage of phase 2, from Early to Middle Jurassic time, SPSs of the outer diapirs of Hennstedt and Honigsee continued to subside. Here, a maximum of 1300 m of Early Jurassic and 1100 m of Middle Jurassic sediments accumulated (Fig. 5f). Thinning of Keuper and Lower to Middle Jurassic strata over the Plön salt pillow denotes the occurrence of an uplifted pillow crest until the beginning of the Early Cretaceous. Different from the innermost salt structures, SPSs of the outer salt structures (Hennstedt, Tellingstedt–Pahlhude, Honigsee) are first deeper on their inner sides. Later, the main depocentres in the SPSs switch to the outer sides of these salt structures.

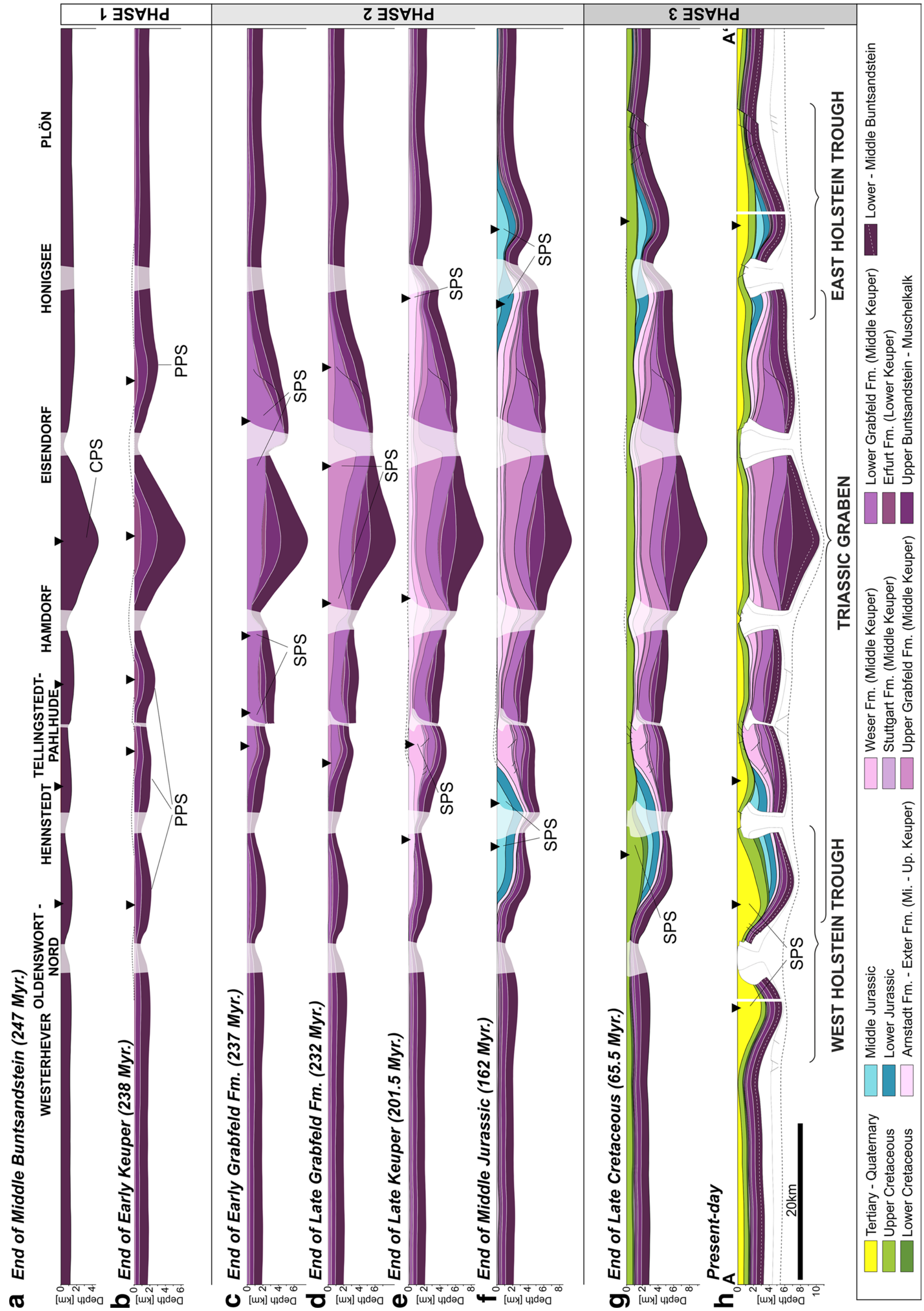
PHASE 1
PHASE 2
PHASE 3
a End of Middle Buntsandstein (247 Myr.)
b End of Early Keuper (238 Myr.)
c End of Early Grabfeld Fm. (237 Myr.)
d End of Late Grabfeld Fm. (232 Myr.)
e End of Late Keuper (201.5 Myr.)
f End of Middle Jurassic (162 Myr.)
g End of Late Cretaceous (65.5 Myr.)
h Present-day
A
A'
Depth [km]
WESTERHEVER
OLDENSWORT - NORD
HENNSTEDT
TELLINGSTEDT- PAHLHUDE
HAMDORF
EISENDORF
HONIGSEE
PLÖN
CPS
PPS
SPS
20km
WEST HOLSTEIN TROUGH
TRIASSIC GRABEN
EAST HOLSTEIN TROUGH
Tertiary - Quaternary
Upper Cretaceous
Lower Cretaceous
Middle Jurassic
Lower Jurassic
Arnstadt Fm. - Exter Fm. (Mi. - Up. Keuper)
Weser Fm. (Middle Keuper)
Stuttgart Fm. (Middle Keuper)
Upper Grabfeld Fm. (Middle Keuper)
Lower Grabfeld Fm. (Middle Keuper)
Erfurt Fm. (Lower Keuper)
Upper Buntsandstein - Muschelkalk
Lower - Middle Buntsandstein

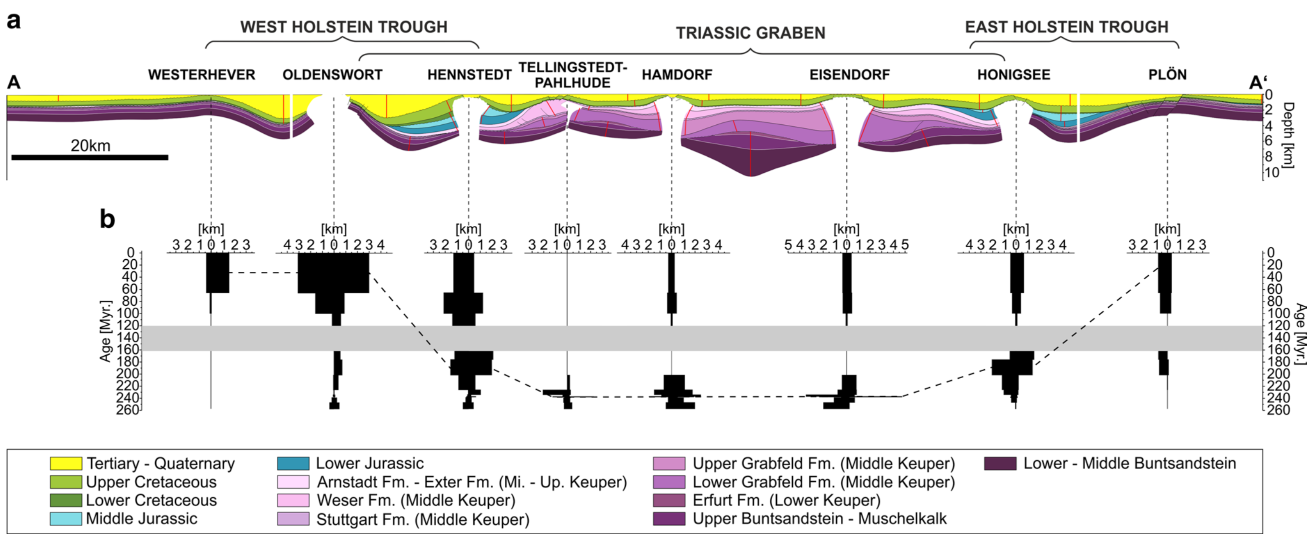

Fig. 6 Timing and amounts of growth of the salt structures in the Glückstadt Graben related to the geological cross section. **a** Geological cross section through the Glückstadt Graben. **b** Diagrams displaying amounts of salt structure growth (*black bars*) calculated from the depth of peripheral sinks on both sides (*red lines* in **a**). The *grey shaded interval* marks the hiatus during the Late Jurassic–Early Cretaceous. The *dashed line* connects phases of maximum growth of each salt structure through time

Third phase: Early Cretaceous to present

After a hiatus from the Late Jurassic to the beginning of the Early Cretaceous, Lower Cretaceous strata (mainly Barremian-Hauterivian) with an almost constant thickness of 80–90 m were deposited across the crests of the inner diapirs (Fig. 5g). Only in the vicinity of the Hennstedt diapir, Lower Cretaceous layers onlap the diapir flanks and form minor SPSs. During the Late Cretaceous, regional sedimentary thickness is 700–1000 m on average. Increased layer thicknesses (~2200 m) were found in the SPS of the Hennstedt diapir. Furthermore, Upper Cretaceous strata are slightly thinned and truncated above the crests of the other diapirs. This indicates uplift of the tops of the diapirs at the end of the Late Cretaceous.

During the Cenozoic, SPSs only formed next to the outer salt wall Oldenswort (West Holstein Trough) with a max. depth of 3100 m. The outer SPS is at the same time the PPS of the outermost salt pillow Westerhever, which began to form in Cenozoic times. Besides the deeply subsided West Holstein Trough, Cenozoic sediments are also slightly thickened between the inner and the eastern salt structures and symmetrically thinned towards the diapirs' crests. Similar to earlier PPSs, this indicates uplift of the diapir roofs (Fig. 5h).

Growth of salt structures

Lateral thickness variations indicate that all salt structures in the Glückstadt Graben except the outermost salt pillows were initiated during Phase 1 (Fig. 6). The innermost salt structures Tellingstedt-Pahlhude, Hamdorf and Eisendorf show their strongest growth during the beginning of Grabfeld Fm. time. The growth of these structures then gradually slowed until the end of the Triassic. In contrast, uplift of the westernmost salt structures of Oldenswort and Hennstedt slowed down after its initiation in Early–Middle Triassic time. The uplift of the Hennstedt diapir was reanimated during Weser Fm. time and reached its maximum during the Early Jurassic, contemporaneous with the strongest uplift of the easternmost diapir Honigsee. This stage was accompanied by the initiation of the easternmost salt pillow of Plön. For the Late Jurassic, amounts of growth are indeterminable owing to the lack of sediments of this age. The Hennstedt and Oldenswort diapirs reveal growth during Early Cretaceous time, possibly indicating continuous rise since the Late Triassic. The uplift of the Oldenswort salt structure reached its maximum during the Cenozoic, accompanied by the initiation of the westernmost salt pillow Westerhever.

Overall, the main phases of salt structure growth became younger with increasing distance from the centre of the Glückstadt Graben (dashed line, Fig. 6). On average, the diapirs spent between 50 and 100 million years in a passive downbuilding stage.

Subsidence curves

Subsidence curves are presented for several characteristic peripheral sinks (Fig. 7). Generally, the total subsidence S_{tot} was strongest during Late Permian and Buntsandstein time. During Late Buntsandstein to Muschelkalk time, subsidence slightly decelerated. An additional peak of subsidence occurred in the period from the Erfurt Fm. (Early Keuper) to the Grabfeld Fm. time. Thereafter and until the beginning of the Cretaceous, S_{tot} increased only slightly. Subsidence accelerated again in the entire basin during the Late Cretaceous.

By incorporating subsidence due to salt expulsion into the backstripping procedure, the tectonic subsidence of the base of salt layer S_{tecS} represents the actual tectonic subsidence of the basin. It can be shown that in periods of strong salt expulsion, tectonic subsidence of the base of Buntsandstein S_{tecB} is seemingly higher than S_{tecS}. In contrast, in the period before strong salt expulsion, S_{tecB} is seemingly lower than S_{tecS}. Curves of S_{tecS} reveal two phases of rapid tectonic subsidence: during Buntsandstein time and in the period from Early Keuper to Grabfeld Fm. time. In contrast, S_{tecS} nearly levels off during later phases, in which S_{tecB} is high, i.e. during the Jurassic (profiles 3, 4; Fig. 7), the Late Cretaceous (profile 4) and the Cenozoic (profile 2; Fig. 7).

The ratio between final tectonic subsidence and the final total subsidence S_{tecS}/S_{totS} ranges between ~0.5 on the graben flanks (profile 1; Fig. 7), ~0.4 in profiles in the Triassic graben (profiles 2 and 7; Fig. 7) and ~0.35 in the basin centre (profile 8; Fig. 7). Hence, the percentage of the isostatic component of the total subsidence is lower in the basin centre than at the plateaus. Since there is no evidence for fault activity at the graben plateau, it can be assumed that tectonic subsidence is completely composed of thermal subsidence (50 % of S_{totS}). In contrast, in the basin centre much of the tectonic subsidence is caused by fault-induced subsidence.

Note that Late Jurassic uplift and resulting removal of sediments were not included in the backstripping procedure. The apparent uplift observed in the curve of S_{tec} during the Late Jurassic is caused by sea level fluctuations.

Subsidence rates

Subsidence rates measured in the 1D profiles were projected onto the 2D cross section according to the position of each 1D subsidence profile on the horizontal axis (Fig. 8). During Early to Middle Buntsandstein time, maximum subsidence rates (~850 m/Myr) occurred in the CPS, while subsidence rates were ~250 m/Myr on average above the West Schleswig Block and the East Holstein-Mecklenburg Block. From Late Buntsandstein to Muschelkalk time, subsidence rates decreased. Enhanced subsidence rates can be observed during Early Keuper time with maximum amounts of 550 m/Myr in the CPS. At the beginning of phase 2 (Early to Middle Grabfeld time), highest subsidence rates can be observed for the entire geological history of the Glückstadt Graben with ~2000 m/Myr on average. The eastern SPS of the Eisendorf diapir subsided fastest at a maximum rate of 4600 m/Myr. By contrast, subsidence rates of the outer platforms of the Glückstadt Graben are approximately 200 m/Myr on average. In Late Grabfeld Fm. time, subsidence rates elevated in the CPS and in SPSs of the innermost diapirs (max. 500 m/Myr). Subsidence rates during the deposition of the Weser and Arnstadt Fms. decreased significantly to 100–200 m/Myr on average and maximum 300 m/Myr within the SPS of the Triassic Graben. Lower Jurassic sediments—preserved in the SPS of the outer diapirs—accumulated at maximum rates of 50 m/Myr. Maximal subsidence rates during the Middle Jurassic are slightly higher (max. 80 m/Myr). Including Late Jurassic erosion and the removal of ~800 m (e.g. Littke et al. 2008) of sediments, average subsidence rates can be as high as ~130 m/Myr.

After the Late Jurassic hiatus, subsidence rates remain generally low compared to those of the Triassic. Although deep depocentres formed in the East Holstein and the West Holstein Trough, maximum subsidence rates in these troughs are ~40 m/Myr averaged over the Late Cretaceous and ~35 m/Myr averaged over the Cenozoic. Even if we assume that the main Cenozoic sediment accumulation took place in Paleogene time with a maximum thickness of 3200 m in the West Holstein trough (Maystrenko et al. 2005a), subsidence rates remained lower than ~100 m/Myr.

Discussion

Salt structure evolution

First phase: Early Buntsandstein to Early Keuper time

Phase 1 is characterised by subsidence of primary peripheral sinks and initiation of most salt structures in the Glückstadt Graben. To explain the subsidence of the Central peripheral sink (CPS), Brink et al. (1992) suggested fault-controlled formation of a relatively narrow graben in the basement below the Permian salt layer. We suggest that the normal faults ("cover grabens") in the Buntsandstein and Muschelkalk layers above the graben flanks are decoupled from the basement faults by the thick salt layer (thin-skinned extension, e.g. Jackson and Vendeville 1994; Nalpas and Brun 1993; Stewart 2007) (Fig. 9a).

Layer thinning, erosional unconformities and sedimentary onlap patterns in the vicinity of the present-day salt diapirs (Baldschuhn 1996; Maystrenko et al. 2005a) implicate either the growth of salt pillows assuming that the salt layer was still covered by post-salt sediments, or of immature salt diapirs assuming that the salt structures were in the stage of pillow to diapir transition (Sørensen 1998). We suggest that the formation of cover grabens during phase

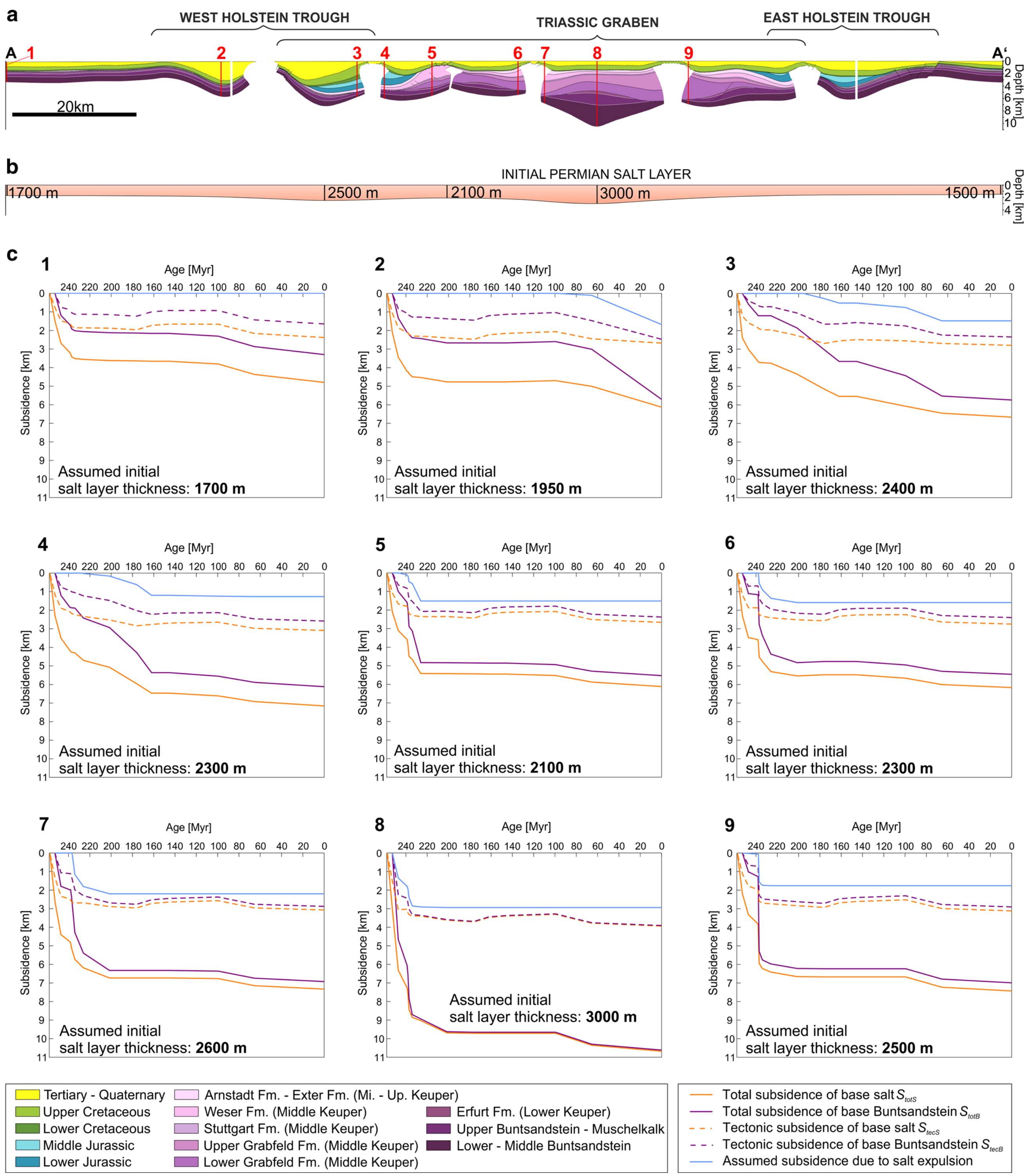

Fig. 7 Subsidence curves for some characteristic peripheral sinks of the Glückstadt Graben. **a** Geological cross section showing locations of the presented subsidence curves. **b** Cross section showing the initial thickness of the Upper Permian salt layer assumed for the 1D backstripping. *Thickness* estimates are according to reconstructions by Maystrenko et al. (2005a). **c** Subsidence profiles showing total subsidence and tectonic subsidence, both for the base of the Buntsandstein layer and the base of the salt layer. The latter was obtained by incorporating the initial salt layer thickness and the temporal reduction of this thickness (*blue curve*) into the backstripping procedure

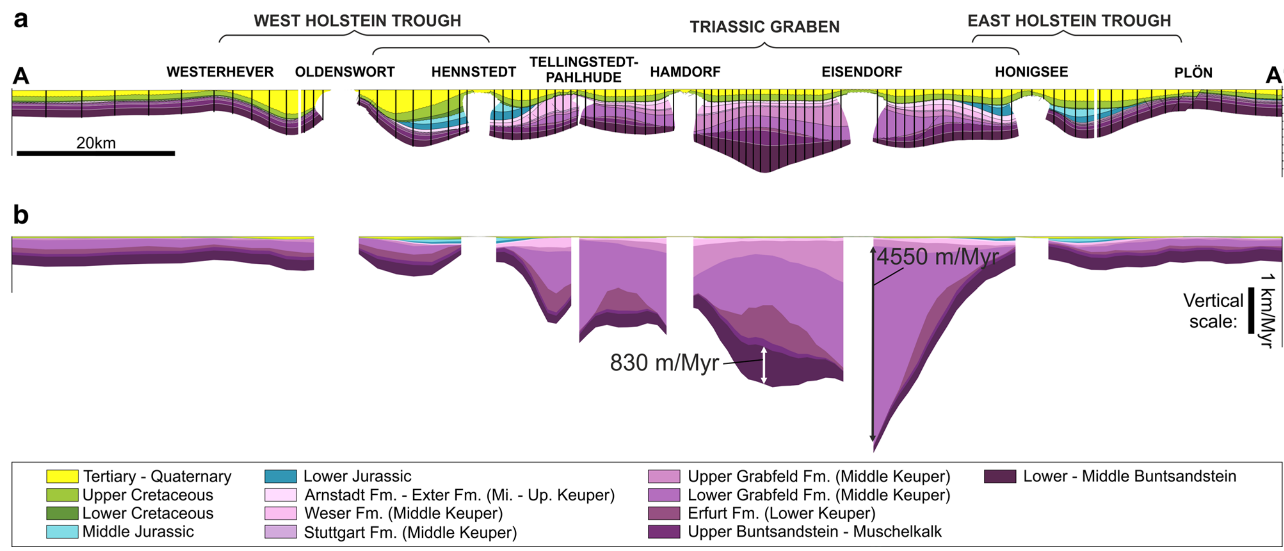

Fig. 8 Subsidence rates in the Glückstadt Graben. **a** Geological cross section including 1D profile used for deriving subsidence data. **b** Average subsidence rates calculated from decompacted layer thicknesses and plotted against x-values of the geological cross section. The 1D profiles are more closely spaced in the centre of the Glückstadt Graben to account for complex thickness variations. Fast regional subsidence occurred during Early–Middle Buntsandstein time. Subsidence was fastest in secondary peripheral sinks during Early–Middle Grabfeld Fm. time. In contrast, subsidence rates in the peripheral sinks of Jurassic, Cretaceous and Cenozoic ages were generally lower

1 created differential loading between regions of extended salt overburden and surrounding regions forcing the salt to flow towards the cover grabens. The innermost salt structures surrounding the CPS showed the highest uplift, as can be inferred from erosional truncation of Buntsandstein and Muschelkalk layers. This resulted from higher differential loading imposed by the CPS compared to relatively low differential loading imposed by the smaller peripheral sinks above the platforms.

Second phase: Middle Keuper time to Middle Jurassic

At the beginning of the Grabfeld Fm. time, the relatively abrupt change in depositional patterns—from the subsidence of PPSs to the formation of SPSs—and the strong increase in subsidence rates can mainly be explained by two processes: (1) Strong basement extension is observed within the entire CEBS during the Late Triassic (Frisch and Kockel 1999; Kockel 2002; Maystrenko et al. 2013). Similarly, enhanced crustal extension is suggested for the Glückstadt Graben (Maystrenko et al. 2005a). Subsidence curves presented here point out that increased tectonic subsidence occurred in particular from Early Keuper until Grabfeld Fm. time. Therefore, it can be suggested that regional extension beginning at the end of phase 1 led to widening of the graben structure (Maystrenko et al. 2005a) and to additional stretching of the cover grabens. (2) Consequently, the transition of the innermost salt structures (Tellingstedt-Pahlhude, Hamdorf and Eisendorf) from pillows or immature diapirs, respectively, into passively growing mature salt diapirs was initiated (Kockel and Krull 1995). Following this transition, flow rates in the salt commonly increased significantly (e.g. Seni and Jackson 1983; Sørensen 1998; Trusheim 1960; Zirngast 1996). Rapid evacuation of the salt beneath the primary sinks caused depletion of the salt layer, progressive rollover of the peripheral sink towards the rising salt diapirs, and eventually the formation of secondary peripheral sinks and turtle-back structures. The absence of SPSs adjacent to the outer salt structures of Hennstedt and Honigsee during Grabfeld Fm. time indicates that these salt structures remained in the pillow or immature diapir stage (Fig. 9b).

The period from Stuttgart Fm. time until the Middle Jurassic is characterised by a lateral shift of the main depocentres from the central trough towards the graben flanks (Fig. 9c, d). However, this migration occurred over a much longer period of time (from 230–162 Myr) than the transition from primary to secondary peripheral sinks during deposition of the Grabfeld Fm. (238–232 Myr). This indicates that the long-lived migration was driven by slow salt expulsion from the basin centre towards the borders of the Glückstadt Graben. At the end of phase 2, the final structural fabric of the salt structures in the Glückstadt Graben was generally arranged (Frisch and Kockel 1999).

Third phase: Early Cretaceous to present

The burial of the inner salt structures by nearly isopachous Lower Cretaceous strata indicates that salt structure uplift over most of the Glückstadt Graben faded out after

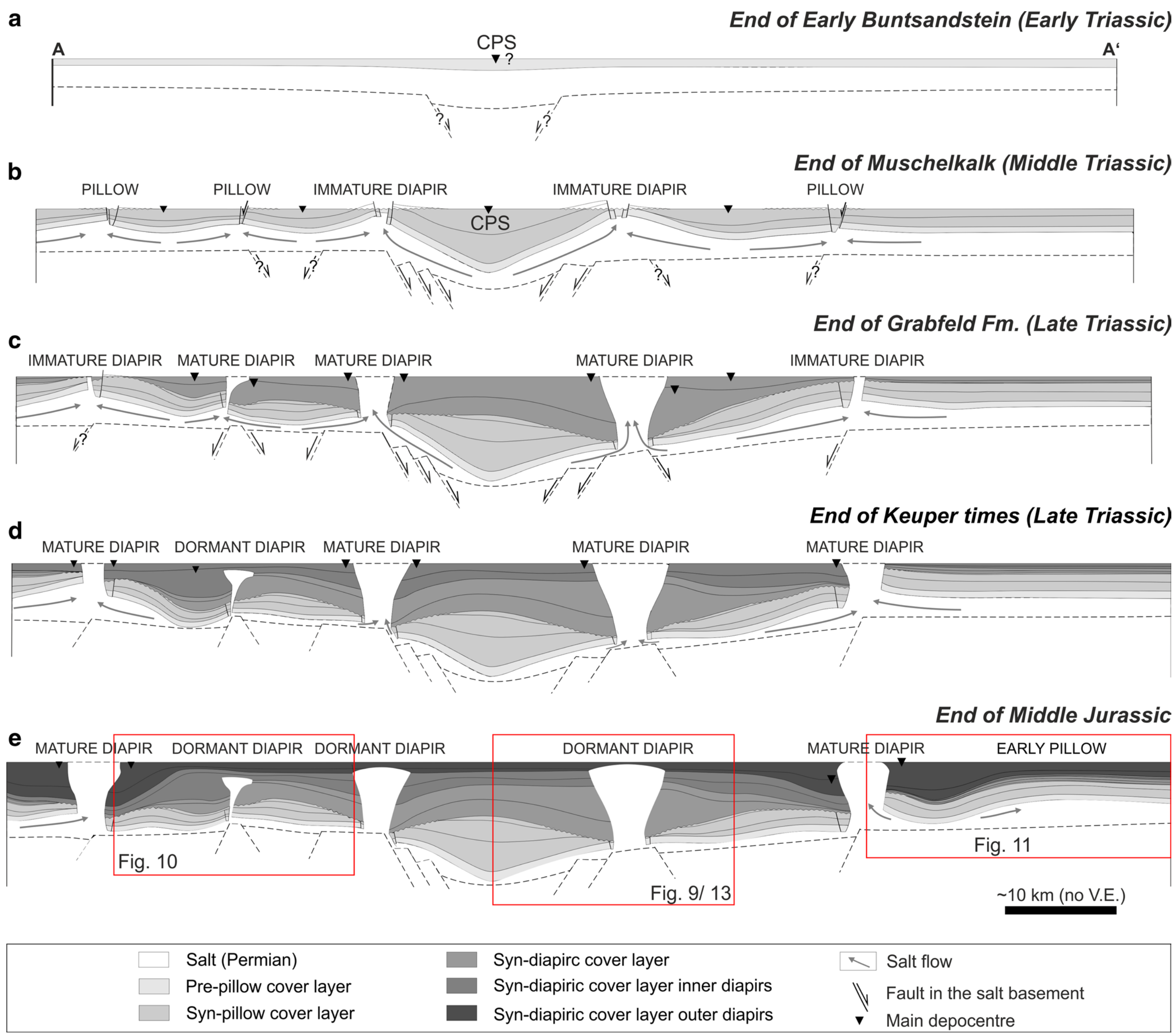

Fig. 9 Conceptual model of salt structure evolution in the Central Glückstadt Graben during phases 1 and 2. **a** Initial stage of the graben. **b** Pillow growth due to basement extension and cover faulting. **c** Phase of basement extension resulting in diapiric piercing of the innermost salt structures. **d** Ongoing basement extension and shifting of the depocentres towards the flanks of the Glückstadt Graben. **e** Main activity of the outer salt walls and decreased activity of the innermost salt walls followed by burial. *Triangles* denote locations of main depocentres. Note that the geometry of the basement and the amount of horizontal stretching of the cross section are speculative

the Middle Jurassic (Fig. 9d). This suggests that the salt layer in the centre of the Glückstadt Graben was already depleted at the end of the Jurassic preventing further salt expulsion. Meanwhile, minor SPSs of Cretaceous age close to the outer salt walls Hennstedt and Oldenswort and thinning of Cretaceous strata towards the Oldenswort salt structure (Maystrenko et al. 2006) implies that the shift of the main depocentres from the centre of the Glückstadt Graben towards its flanks slowly continued in the outer parts of the Glückstadt Graben, where relatively thick salt was left in the source layer.

During the Late Cretaceous and Early Tertiary, diapirs show upwarped and eroded layers as well as the formation of keystone grabens above their crests, which generally indicate squeezing of a salt structure due to lateral contraction (e.g. Dooley et al. 2009). In the Glückstadt Graben, this was interpreted to be due to thin-skinned shortening related to basement-involved shortening (Maystrenko et al. 2006), which affected regions further to the south, e.g. the Lower Saxony Basin (Betz et al. 1987; Baldschuhn et al. 1991) or the Allertal fault zone (Lohr et al. 2007). However, apart from rising diapirs, further indications for shortening of the salt basement and the overburden are lacking in geological profiles (Baldschuhn et al. 2001) and seismic data of the Glückstadt Graben(Maystrenko et al. 2005a). Salt walls of the Glückstadt Graben are generally trending almost parallel to the contraction affecting Central Europe during Late Cretaceous to Early Tertiary time (N-S to NE-SW) (Scheck-Wenderoth and Lamarche 2005; Kley et al. 2008). Squeezing of the salt walls parallel to their long axes thus would also have to affect the surrounding post-salt strata. The link between the Late Cretaceous reactivation of salt movement in the Glückstadt Graben and regional contraction, however, needs further investigation.

During the Tertiary, revived growth of all diapirs can be inferred from layer thinning above the diapirs' crests. Particularly, diapiric piercing of the Oldenswort salt wall and increased uplift of the outermost salt pillows Westerhever and Plön (Kockel and Krull 1995) point to increased salt flowage in the marginal parts of the Glückstadt Graben. According to Maystrenko et al. (2006), this latest stage of growth took place during almost E-W-directed extension in Eocene to Miocene times.

Conceptual model for the migration of the main depocentres

In order to explain the temporal evolution of the salt structures in the Glückstadt Graben, multiple tectonic pulses that induced episodes of strong salt flow (e.g. Maystrenko et al. 2006) were proposed. These phases assumed to be interrupted by periods of arrested salt flow coinciding with tectonic quiescence. Our results confirm that the growth of salt pillows and adjoining PPS as well as pillow to diapir transition of the inner salt structures and subsidence of surrounding SPS were initiated by regional extension during Buntsandstein time or Early Keuper to Grabfeld FM. time, respectively.

However, the growth of salt pillows (from Late Buntsandstein to Early Keuper time) and the rise of passive diapirs (from Upper Grabfeld Fm. time to the end of the Jurassic or longer) further continued until the end of phase 1 or phase 2, respectively. During phase 1, ongoing salt flow can be inferred from the uninterrupted subsidence of peripheral sinks, even though rates of salt flow decreased during Muschelkalk time. During phase 2, subsidence of wedge-shaped secondary peripheral sinks next to the inner salt walls lasted throughout the entire Triassic until the salt layer beneath the peripheral sinks was depleted. Nevertheless, subsidence rates and, therefore, salt flow rates significantly decreased after Grabfeld Fm. time, which is likely because Arnstadt and Exter Fm. times are tectonically quiet periods (Kockel 2002).

The development of SPSs next to the outer salt walls Hennstedt and Honigsee began during Arnstadt Fm. time and continued until the Middle Jurassic (Fig. 4). In seismic data of the Glückstadt Graben, parallel reflections can be observed at the transition from the Triassic to the Jurassic (Maystrenko et al. 2005a, 2006; Baykulov et al. 2009). Only directly adjacent to salt structures, Triassic and Jurassic strata are separated by angular unconformities (Maystrenko et al. 2005a). In other regions of the CEBS, the beginning of Jurassic extension is dated to the Middle Jurassic, e.g. in the Central Graben (e.g. Duffy et al. 2013; Arfai et al. 2014) or in the Lower Saxony Basin (Betz et al. 1987), although some tectonic movements have been suggested for parts of the North German Basin during the Early Jurassic (e.g. Kockel 2002; Maystrenko et al. 2005a; Lohr et al. 2007). However, these tectonic events likely occurred later than the pillow–diapir transition of the outer salt walls Hennstedt and Honigsee. Therefore, we suggest that the structural patterns and the salt flow kinematics in the Glückstadt Graben were not significantly modified by additional tectonic pulses during Weser Fm. time (Frisch and Kockel 1999) or during the Jurassic (Maystrenko et al. 2006).

Our conceptual model proposes that salt flow and the migration of main depocentres during phase 2 and during the late stage of phase 3 were driven by differential loading after being triggered or reactivated by tectonic stresses. As it has been proposed by Sannemann (1968) and shown by analogue models (e.g. Warsitzka et al. 2013, 2015) as well as numerical models (e.g. Peel 2014), the formation of a diapir can lead to expulsion of the source layer towards neighbouring regions and force the formation of new salt structures. In the Glückstadt Graben, extensionally triggered peripheral sinks adjacent to the innermost salt structures might have also forced expulsion of salt towards the neighbouring salt structures. The latter pierced their overburden as soon as differential loading had increased sufficiently to overcome the strength of the overburden or when an additional tectonic pulse thins the cover of the salt pillows (cf. Hudec and Jackson 2007). Subsequent to piercing, additional SPSs formed adjacent to the younger salt diapirs.

The process of migration of the main depocentres and salt expulsion from beneath the SPS to the outer parts of the Glückstadt Graben significantly slowed after the Middle Jurassic. This can be attributed to three factors: (1) the initial thickness of the salt layer decreases towards the grabens flanks (Maystrenko et al. 2005a), which generally reduces flow velocities of the salt. (2) Due to the hiatus and erosion from the Late Jurassic to the Early Cretaceous, sediment accumulation in peripheral sinks ceased. Hence, the increase in load required for further salt expulsion was cut off. (3) Tectonic tranquillity was interpreted for the Glückstadt Graben during this time (Maystrenko et al. 2006), suggesting that fault-induced salt tectonics did not occur.

Major reactivation of salt flow and salt structure growth occurred not until the Late Cretaceous(?) and Cenozoic, when regional deformation again affected the Glückstadt Graben.

Structural characteristics of the peripheral sinks in the Glückstadt Graben

Typical structural features evolved in the peripheral sinks due to the expulsion of the salt layer will be discussed here.

1. Graben centre diapirs: The innermost diapirs (Hamdorf, Eisendorf) flank the CPS, which represents the main primary peripheral sinks of these salt walls (Fig. 10a). However, the deepest *secondary* peripheral sinks of these diapirs developed on their outer sides during deposition of the Lower Grabfeld Fm. (Fig. 10b). This switching of peripheral sinks from one side of the diapir to the other could either be explained by the activation of outward dipping normal faults beneath the SPSs of the diapirs, or by varying salt movement. The first option requires the formation of a fault underlying the outer SPS. However, there is no indication for basement normal faults with sufficiently large offsets (>1000 m) dipping away from the graben centre either in the original seismic profile used here (Baldschuhn 1996) or in other profiles (Baldschuhn et al. 2001) trending parallel to our cross section. The second option considers salt expulsion and salt extrusion close to the deep SPS as follows: At the beginning of the diapiric breakthrough (phase 1), salt was supplied to the innermost salt structures of the Glückstadt Graben mainly from beneath the CPS (Fig. 10a). This forced relative uplift of the inner flanks of these salt structures and probably salt extrusion on top of the outer flanks. These salt extrusions can produce topography above the general sedimentary surface (Fig. 10b), thus increasing the loading and the subsidence of the outer SPSs. This mechanism may also help to explain the enormous subsidence rates (>4000 m/Myr) characterising the SPSs of the innermost salt structures during Lower to Middle Grabfeld Fm. time. Salt extrusion as well as surficial dissolution and re-precipitation of Permian salt led to the accumulation of significant thicknesses of evaporites in the SPS (especially during Grabfeld and Weser Fm. time). Such surficial outflow of Permian salt in the North German Basin was proven by detecting Permian microfossils in younger evaporites of Triassic and Jurassic age (Trusheim 1960) and recognising buried salt extrusion (salt glaciers) in seismic profiles located south of the Glückstadt Graben (Mohr et al. 2007). Evaporites have relatively high densities (e.g. halite: 2.04 kg/m^3, anhydrite: 2.98 kg/m^3 (Urai et al. 2008)) compared to less compacted clastic sediments near the surface (1.5–1.8 kg/m^3) (Jackson and Talbot 1986). Consequently, the loading induced by evaporites in peripheral sinks is significantly higher than that of clastics, which accelerated subsidence of SPSs in Grabfeld Fm. time. Combined with a sudden acceleration of tectonic subsidence and isostatic response to the sediment load (Fig. 6), total subsidence rate can reach unusually high values.
2. Platform diapirs: Diapirs located at a distance from the CPS (Hennstedt, Tellingstedt-Pahlhude, Honigsee) are characterised by asymmetric peripheral sinks similar to the graben centre diapirs. However, the main peripheral

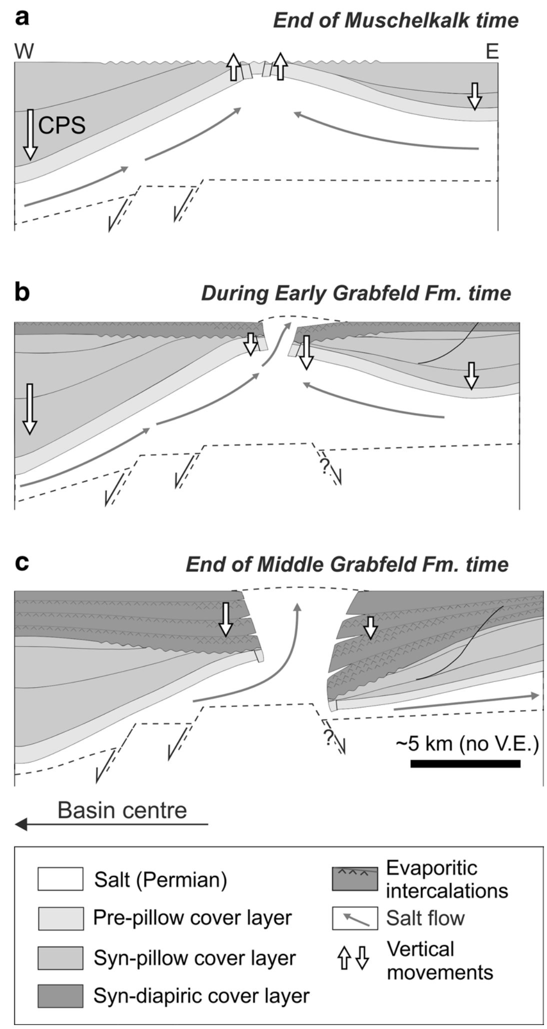

Fig. 10 Structural evolution of secondary peripheral sinks of a graben centre diapir in the Glückstadt Graben. **a** Strong subsidence of the central peripheral sink during phase 1 causes salt flow mainly from hanging wall side. **b** During and after piercing of the diapir in phase 2, salt upwelling forces slower subsidence of the inner flanks of the diapir compared to the outer flanks. **c** After depletion of the salt layer beneath the outer secondary peripheral sink, main depocentre switches back to the inner side of the downbuilding diapir

sinks of the platform diapirs switched multiple times from one side of the diapirs to the other (Fig. 4). This change in structural polarity of the peripheral sinks has been termed as "flip-flop salt tectonics" (Quirk and Pilcher 2012). Various mechanisms might be responsible for this behaviour: (1) During phase 1, differential subsidence of the overlying peripheral sinks can be caused by temporarily varying activity of oppositely dipping basement faults beneath the diapirs or by a succession of thin-skinned extension linked to the central graben and subsequently thick-skinned extension linked to basement faults beneath the salt structures (Fig. 11b). (2) During phase 2, a lateral shift of depocentres from the inner diapirs towards the outer diapirs can lead to asymmetric salt expulsion beginning at the inner side of the platform diapir (Fig. 11c) and later switching to the outer side of the diapir (Fig. 11d). (3) A further explanation could be the progradation of sedimentary wedges. As shown by analogue experiments (Ge et al. 1997), sediment propagation leads to asymmetric peripheral sinks next to squeezed out diapirs. However, the progradation of large sedimentary wedges in Keuper time is unlikely for the area of the Glückstadt Graben, since sedimentation at that time was dominated by evaporitic and playa lake facies (Barnasch 2010). These facies types are characterised by aggradation rather than progradation.

3. Basin-edge pillows: The Glückstadt Graben is bounded by elongated salt pillows, in regions showing no indications for cover faults of Triassic age (Fig. 12). These pillows formed at the outer edges of the West Holstein Trough and the East Holstein Trough as a consequence of the subsidence of peripheral sinks mainly during the Tertiary (Maystrenko et al. 2006). They remained in the pillow stage probably because the overburden of Triassic to Cretaceous age was too thick to allow diapiric breakthrough. However, geological cross sections south of the section presented here show that the salt intruded the cover layer through a normal fault formed during the Tertiary (Baldschuhn et al. 2001). This represents a possible example of a salt structure in the transition from pillow to diapir.

Limitations of the reconstruction

Technical uncertainties

The seismic interpretation of the geological cross section used here could have been affected by the following technical problems:

1. The correlation of stratigraphic horizons in the seismic data from outside the graben towards the graben centre basin may be partly inaccurate. This is because the quality of the data underlying the Geotectonic Atlas of Northern Germany (Baldschuhn 1996) is heterogeneous (Hese 2012), and seismic energy is lost with depth resulting in insufficient resolution especially of deeply buried (up to 11 km) Triassic strata in the basin centre that were never drilled (Maystrenko et al. 2005b). The corresponding lack of information about the petrophysical parameters of the rocks in the basin centre may have led to incorrect velocity models resulting in inaccurate depth migration of the seismic data.

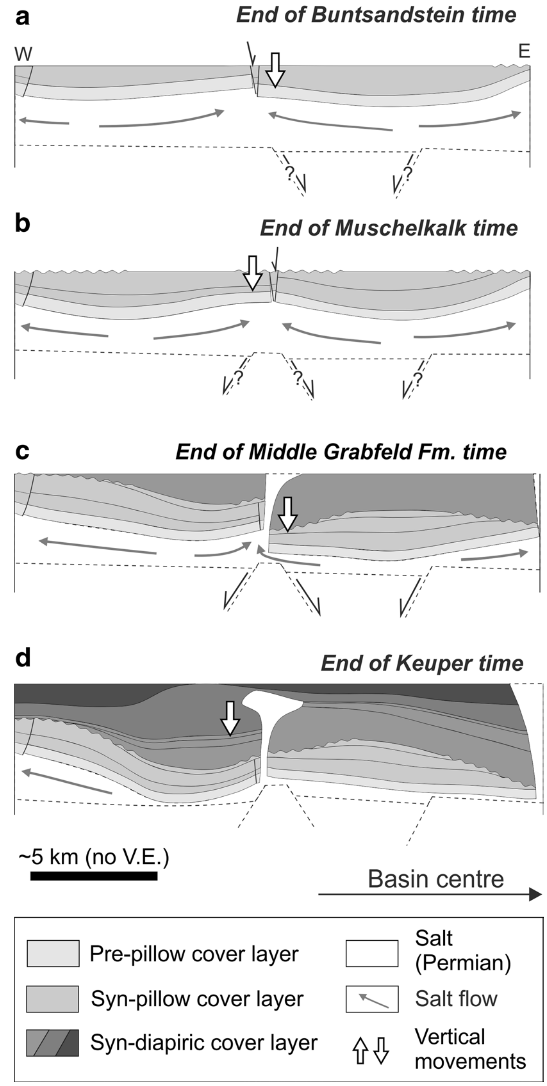

Fig. 11 Structural evolution of secondary peripheral sinks of a platform diapir in the Glückstadt Graben: Multiple switching of main depocentres adjacent to the diapir Tellingstedt-Pahlhude. **a** During Buntsandstein time, thin-skinned extension cause the initiation of PPSs. **b** Main depocentre shifts towards the outer side of the salt structure. **c** Further extension leads to piercing of the salt structure, whereas the deeper SPS develops at the inner side of the diapir. **d** During the Late Triassic, the main SPS shifts to the outer side possibly after salt welding beneath the inner side SPS

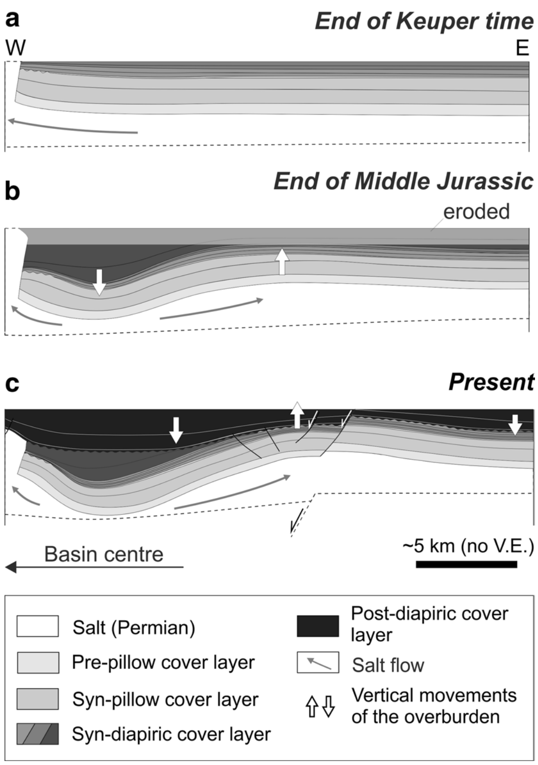

Fig. 12 Structural evolution of the basin-edge pillow Plön. **a** Pillow to diapir transition of the platform diapir (Honigsee). **b** Subsidence of the outer SPS of the downbuilding diapir cause salt expulsion towards the basin edges and the beginning of pillow uplift. **c** Slow growth continues during the Cretaceous. Tertiary extension leads to faulting of the pillow crest and increased growth of the pillow

2. The presence of salt structures and of salt layers in post-Permian successions (e.g. in the Middle Keuper) impairs seismic imaging beneath the salt bodies, since much of the seismic energy is lost at the boundary of the salt (Leveille et al. 2011; Jones and Davison 2014). Furthermore, seismic imaging in the vicinity of salt diapirs boundaries is poor, because of the steeply dipping and mostly irregular boundary of salt diapirs, salt overhangs at the heads of diapirs, or faults and folds in the post-salt strata around them. For instance, the Lower Buntsandstein to Middle Keuper succession may be dissected by normal faults as shown in Fig. 9. For these reasons, offsets of basement faults beneath salt diapirs as well as onlap geometries and thickness variation of post-salt layers in the vicinity of the salt walls are prone to high uncertainties. According to other interpretations of salt structures in Northern Germany (e.g. Baykulov et al. 2009; Mohr et al. 2005; Kukla et al. 2008), the shapes of the salt diapirs are usually much more irregular than the straight vertical salt wall boundaries interpreted in the cross section used here (Fig. 2). New techniques of stacking (e.g. common reflection surface stacking) applied to the seismic data of the Glückstadt Graben improved the seismic imaging of the layered sedimentary successions (Baykulov et al. 2009; Yoon et al. 2009). This revealed that the width of the diapirs in the Glückstadt Graben might be much smaller than interpreted in Baldschuhn (1996). Consequently, the salt volume and, thus, potential subsidence due to salt expulsion are overestimated. Furthermore, the widths of the peripheral sinks also carry errors of several hundreds of metres. However, seismic reflectors between the salt walls are relatively well imaged. Therefore, structural geometries in the centre of the peripheral sinks can be reconstructed reliably by the method applied here.
3. The stratigraphic resolution of the post-Triassic layers is low. Therefore, extensional phases, e.g. during the Jurassic or Cenozoic, might be levelled out in the subsidence data, which prevents a more detailed reconstruction of the post-Triassic subsidence history.

Overall, these technical issues point to the necessity of a new processing and interpretation of the seismic data, but this is beyond the scope of this study.

Uncertainties caused by geological processes

1. Erosional unconformities adjacent to or above salt structures (Fig. 2) may lead to underestimations of original layer thicknesses and, therefore, underestimations of compaction and decompacted thickness of the underlying layers. In particular, erosion of pillow crests during the transition from phase 1 to phase 2 (end of Early Keuper time) might amount to several hundreds of metres (Fig. 9). However, since the exact values are unknown, eroded parts of the layers were not reconstructed.
2. Mobile evaporitic rocks intercalated in the Triassic strata (Grabfeld Fm. and Weser Fm.) could be affected by post-depositional salt flow. In the southern part of the Glückstadt Graben, mobile halite layers in the Upper Triassic Weser Fm. can be as thick as 2400 m. A part of this thickness is attributed to the formation of salt pillows (Frisch and Kockel 1999). Unfortunately, there are no further quantifications of ductile deformations in the post-Permian salt layers.
3. The intrusion of Permian salt into younger evaporitic layers (e.g. Upper Buntsandstein or Middle Keuper) can increase the thickness of the peripheral sinks. Such intrusions with a maximum thickness of 700 m were interpreted in seismic profiles from the northern part of the Glückstadt Graben (Baldschuhn 1996). Salt intrusions are assumed to be caused by compres-

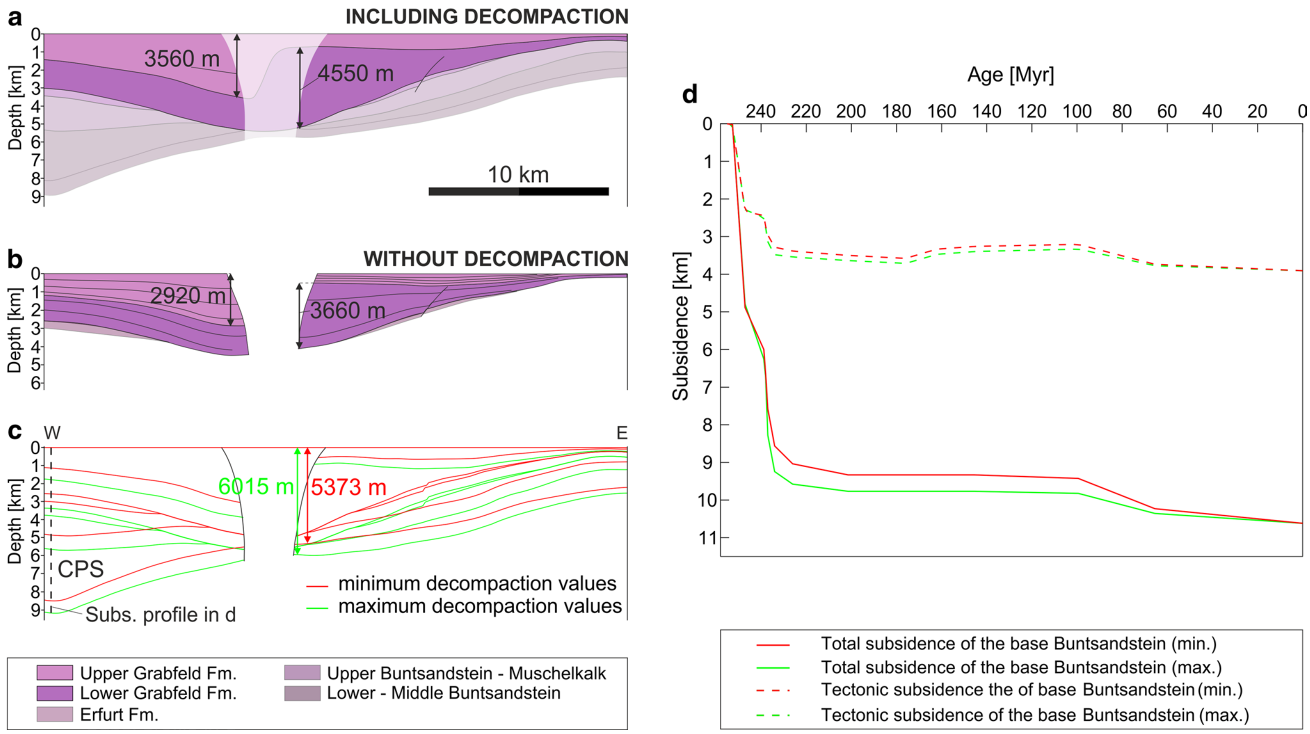

Fig. 13 Variations of decompacted layer thicknesses and subsidence curves depending on applied decompaction parameters (Table 1). **a** Structural reconstruction of the SPSs next to the Eisendorf salt wall (end of Grabfeld Fm. time) applying decompaction parameters according to the average lithological composition of the stratigraphic units. **b** Reconstruction of the Lower to Upper Grabfeld Fm. without applying decompaction (modified after Baldschuhn 1996). **c** Reconstruction showing differences in decompacted layer thicknesses related to minimum and maximum decompaction parameters in the sensitivity study. **d** Subsidence curves of the CPS (profile 8, Fig. 7) showing differences in the total subsidence and the tectonic subsidence of the base Buntsandstein

Table 2 Difference in total subsidence S_{totB}, tectonic subsidence S_{tecB} and subsidence rate of the base Buntsandstein using maximum or minimum decompaction parameters (Table 1)

Unit/formation	Age of top (Myr)	Difference in S_{totB} (m)	Difference in S_{tecB} (m)	Difference in subsidence rate (m/Myr)
Tertiary + Quaternary	0	0	0	0
Upper Cretaceous	65.5	127	35.6	3.7
Lower Cretaceous	99.5	398	125.8	8.7
Upper Jurassic	145.5	–	–	–
Middle Jurassic	162	–	–	–
Lower Jurassic	176	–	–	–
Arnstadt-Exter Fm. (Middle-Upper Keuper)	201.5	437	137.4	17.8
Weser Fm. Middle Keuper	226	540	154.0	67.5
Upper Grabfeld Fm. (Middle Keuper)	234	682	200.4	227.3
Lower–Middle Grabfeld Fm. (Middle Keuper)	237	698	195.6	698.0
Erfurt Fm. (Lower Keuper)	238	87	14.5	108.7
Upper Buntsandstein–Muschelkalk	238.8	256	37.0	30.8
Lower–Middle Buntsandstein	247.1	−94	−33.0	−16.8

Example is calculated for subsidence profile 8 (see Fig. 7 for location) sion or transpression of a previously formed diapir (Baldschuhn et al. 1998). In the Glückstadt Graben, this requires a post-Triassic phase of compression or transpression—probably in the Late Cretaceous (Coniacian to Campanian; Baldschuhn et al. 1998).

4. Besides technical issues with defining the salt basement (see above), it is also problematic to sharply define the basement beneath the Permian salt in terms of mechanical behaviour. This is because Rotliegend (Permian) evaporites are involved in the salt diapirism in the centre of the Glückstadt Graben, whereas the Rotliegend strata in the outer parts of the Glückstadt Graben are undisturbed by salt movement (Maystrenko et al. 2005a). The lower mobility of the Upper Rotliegend succession away from the graben centre probably reflects a gradual increase in the proportion of shale.

Uncertainties of the decompaction procedure, in particular of the decompaction values (initial porosity data and depth coefficient) can result from the following factors:

1. The decompaction procedure applied does not include the effects of cementation of the pore space, which usually reduces mechanical compaction. This has to be considered especially for sandstones of the Buntsandstein and the Keuper (e.g. Stuttgart Fm.), which locally possess porosities of 25–35 % (including cemented pore space) in the CEBS (e.g. Purvis and Okkerman 1996; Wolfgramm et al. 2008). The state of compaction in the Glückstadt Graben, e.g. in the CPS, cannot be verified owing to the lack of well data.
2. Lateral and vertical lithological variations within a stratigraphic horizon cause uncertainties in the average decompaction values used here, e.g. the ratio between claystones and evaporites within the Grabfeld Fm. might change from the deep peripheral sinks in the basin centre to the platforms at the basin margin.

Sensitivity study

In order to test the influence of varying decompaction values, a sensitivity study was carried out setting minimum and maximum values for initial porosity and depth coefficient (Table 1). This yields a range of possible subsidence values exemplarily shown in Fig. 13 and Table 2. Variations of the total subsidence of as much as 30 to 130 m can be stated for the Lower to Middle Buntsandstein layer along the cross section (Table 2). Consequently, the error of subsidence rates during this interval is ~15–25 m/Myr. Larger differences in the total subsidence result for Middle and Upper Triassic strata, e.g. for the Lower to Upper Grabfeld Fm.. Differences range between 100 m in the outer parts of the Glückstadt Graben and up to 800 m in the deepest SPSs in the centre of the Glückstadt Graben. These large variations are due to the large absolute thickness of these layers and due to the large differences between the applied maximum and minimum values of the decompaction parameters (Table 1).

The abnormally high subsidence rates calculated for the Lower to Middle Grabfeld Fm. (>4000 m/Myr, Fig. 8) can be partly explained by poorly constrained decompaction parameters. However, palinspastic reconstructions (without applying decompaction) of the Keuper layers shown in the GTA (Baldschuhn 1996) yielded a maximum thickness of 3660 m for the Lower to Middle Grabfeld Fm. (Fig. 13b). This results in a similarly high subsidence rate (3660 m/Myr). Even when taking into account errors in the correlation of stratigraphic boundaries and the technical limitations discussed above (e.g. erroneous correlations of seismic reflectors), max. subsidence rates during Lower–Middle Grabfeld Fm. time remain significantly higher (~ 2000–3000 m/Myr) than in any other post-Permian phase in the Glückstadt Graben.

Conclusions

Based on a key geological cross section through the central Glückstadt Graben (Northern Germany), the growth of salt diapirs and subsidence of adjacent peripheral sinks were reconstructed using decompaction and backstripping. On the basis of these reconstructions, three phases of salt structure evolution can be distinguished:

1. Most salt structures were initiated by basement faulting in the period from Early to Middle Buntsandstein time (Early Triassic). Regional extension caused normal faulting in the centre of the Glückstadt Graben leading to thickness variations in the overburden of the Permian salt layer. From Late Buntsandstein to Early Keuper time, salt pillows or immature salt diapirs evolved accompanied by subsidence of primary peripheral sinks.
2. At the beginning of Keuper time, regional extension induced a major change in depositional patterns. An abrupt switch from primary to secondary peripheral sinks occurred adjacent to the innermost salt structures of the Glückstadt Graben. Extremely high subsidence rates in the time of the Grabfeld Formation (up to 4500 m/Myr) points to fast regional extension, strong salt flow and diapiric breakthrough in the centre of the Glückstadt Graben.

The interval from Late Grabfeld Fm. time to the Middle Jurassic was a long-lasting phase of salt flow and downbuilding of the diapirs. The main depocentres gradually migrated outwards from the graben centre towards the flanks. We suggest that this lateral shift was mainly caused by the expulsion of salt from salt diapirs towards their neighbouring salt structures, but was modulated and accelerated by phases of regional extension, e.g. during the Late Triassic (Weser Fm.) or the Jurassic.

3. After a phase of regional erosion (Late Jurassic–Early Cretaceous), salt movement and the growth of the inner salt walls ceased. Minor salt structure growth only continued at the margins of the Glückstadt Graben. The growth of the inner salt structures and especially of salt walls and salt pillows in the West Holstein Trough and in the East Holstein Trough was renewed during Late Cretaceous probably due to shortening and in particular during Tertiary due to regional extension.

Depending on their location, the peripheral sinks of the Glückstadt Graben exhibit characteristic structural features:

1. The innermost diapirs bounding the graben centre possess very deep secondary peripheral sinks filled by the Middle Keuper Grabfeld Formation. These peripheral sinks developed on the outer sides of the diapirs, facing away from the graben centre. This phenomenon can be explained by strong salt expulsion from beneath the central peripheral sinks, which caused relative uplift of the inner flanks of the innermost diapirs and salt expulsion onto the outer flanks.
2. The peripheral sinks of the outer diapirs located above the graben flanks switched multiple times from one side of a diapir to its other side. We suggest that this switching was related to variable basement faulting, changing directions of salt influx and the influence of salt expulsion from neighbouring salt walls.
3. The salt structures above the outer swells of the graben remained in the pillow stage and possess only one deep primary peripheral sink. The piercing of these pillows was probably prevented by the large thickness of the post-Permian sediments.

Acknowledgments Funding for Michael Warsitzka came from the Federal Ministry of Education and Research (BMBF) (Grant No. 03IS2091A INFLUINS) and the German Academic Exchange Service (DAAD). We gratefully acknowledge Midland Valley for providing free university licences of 2DMOVE™. We have benefited from helpful discussion with T. Voigt. Reviewers P. Kukla and Y. Maystrenko are thanked for valuable comments improving the contents and presentation of our paper.

References

Allen PA, Allen JR (2013) Basin analysis: principles and application to petroleum play assessment. Wiley, New York

Arfai J, Jähne F, Lutz R, Franke D, Gaedicke C, Kley J (2014) Late Palaeozoic to Early Cenozoic geological evolution of the northwestern German North Sea (Entenschnabel): new results and insights. Neth J Geosci 93(04):147–174

Athy LF (1930) Density, porosity, and compaction of sedimentary rocks. AAPG Bull 14(1):1–24

Bachmann GH, Grosse S (1989) Struktur und Entstehung des Norddeutschen Beckens - geologische und geophysikalische Interpretation einer verbesserten Bouguer-Schwerekarte. Nds Akad Geowiss Veröfftl 2:23–47

Baldschuhn R (1996) Geotektonischer Atlas von Nordwest-Deutschland und dem deutschen Nordsee-Sektor. Hannover

Baldschuhn R, Best G, Kockel F (1991) Inversion tectonics in the north-west German basin. Generation, accumulation, and production of Europes hydrocarbons. Spec Publ Eur Assoc Petroleum Geosci 1:149–159

Baldschuhn R, Frisch U, Kockel F (1998) Der Salzkeil, ein strukturelles Requisit der saxonischen Tektonik. Zeitschrift der deutschen geologischen Gesellschaft, pp 59–69

Baldschuhn R, Binot F, Fleig S, Kockel F (2001) Geotektonischer Atlas von Nordwest-Deutschland und dem deutschen Nordsee-Sektor. Hannover

Barnasch J (2010) Der Keuper im Westteil des Zentraleuropäischen Beckens (Deutschland, Niederlande, England, Dänemark): diskontinuierliche Sedimentation, Litho- , Zyklo- und Sequenzstratigraphie. Schriftenreihe der Deutschen Gesellschaft für Geowissenschaften, pp 7–169

Bayer U, Maystrenko Y, Hoffmann N, Scheck-Wenderoth M, Meyer H (2003) 3D structural modelling and basin analysis of the Central European Basin System (CEBS) between the North Sea and Poland. Terra Nostra 3:1–4

Baykulov M, Brink HJ, Gajewski D, Yoon MK (2009) Revisiting the structural setting of the Glueckstadt Graben salt stock family. North German basin. Tectonophysics 470(1):162–172

Best G, Kockel F, Schöneich H (1983) Geological history of the southern Horn Graben. In: Petroleum geology of the southeastern North Sea and the adjacent onshore areas. Springer, pp 25–33

Betz D, Führer F, Greiner G, Plein E (1987) Evolution of the Lower Saxony basin. Tectonophysics 137(1):127–170

Beutler G (2005) Stratigraphie von Deutschland, vol 4. E. Schweizerbart'sche, Verlagsbuchhandlung

Bishop DJ, Buchanan PG, Bishop CJ (1995) Gravity-driven thin-skinned extension above Zechstein Group evaporites in the western central North Sea: an application of computer-aided section restoration techniques. Mar Pet Geol 12(2):115–135

Brink H, Dürschner H, Trappe H (1992) Some aspects of the late and post-Variscan development of the Northwestern German Basin. Tectonophysics 207(1):65–95

Buchanan PG, Bishop DJ, Hood DN (1996) Development of salt-related structures in the Central North Sea: results from section balancing. Geol Soc Lond Spec Publ 100(1):111–128

Dooley TP, Jackson MPA, Hudec MR (2009) Inflation and deflation of deeply buried salt stocks during lateral shortening. J Struct Geol 31(6):582–600

Doornenbal JC, Stevenson AG (2010) Petroleum geological atlas of the Southern Permian basin area. Houten, Netherlands, European Association of Geoscientists & Engineers

Duffy OB, Gawthorpe RL, Docherty M, Brocklehurst SH (2013) Mobile evaporite controls on the structural style and evolution of rift basins: Danish Central Graben, North Sea. Basin Res 25(3):310–330

Frisch U, Kockel F (1999) Quantification of early Cimmerian movements in NW-Germany. Zentralblatt Geol Paläontol I 7:571–600

Gast R, Gundlach T (2006) Permian strike slip and extensional tectonics in Lower Saxony, Germany. Zeitschrift der deutschen Gesellschaft für Geowissenschaften 157(1):41–55

Ge H, Jackson MPA, Vendeville BC (1997) Kinematics and dynamics of salt tectonics driven by progradation. AAPG Bull 81(3):398–423

Haq BU, Hardenbol J, Vail PR (1987) Chronology of fluctuating sea levels since the Triassic. Science 235(4793):1156–1167

Hese F (2012) 3D-Modellierungen und Visualisierung von Untergrundstrukturen für die Nutzung des unterirdischen Raumes in Schleswig-Holstein. Christian-Albrechts-Universitat, Kiel

Hossack J (1995) Salt tectonics: a global perspective: based on the Hedberg international research conference, Bath, UK, September 1993. In: Jackson M, Roberts D, Snelson S (eds) Salt tectonics: a global perspective, AAPG memoir, vol 65, American Association of Petroleum Geologists, pp 29–40

Hudec MR, Jackson MPA (2007) Terra infirma: understanding salt tectonics. Earth Sci Rev 82(1):1–28

Hudec MR, Jackson MPA (2011) The salt mine: a digital atlas of salt tectonics, vol 99. Bureau of Economic Geology Udden Book Series No. 5

Jackson MPA, Talbot CJ (1986) External shapes, strain rates, and dynamics of salt structures. Geol Soc Am Bull 97(3):305–323

Jackson MPA, Vendeville BC (1994) Regional extension as a geologic trigger for diapirism. Geol Soc Am Bull 106(1):57–73

Jaritz W (1987) The origin and development of salt structures in Northwest Germany. In: O'Brien I, Lerche J (eds) Dynamical geology of salt and related structures. Academic Press, Cambridge, pp 479–493

Jaritz W, Best G, Hildebrand G, J U (1991) Regionale Analyse der seismischen Geschwindigkeiten in Nordwestdeutschland. Geologisches Jahrbuch E 45:23–57

Jones IF, Davison I (2014) Seismic imaging in and around salt bodies. Interpretation 2(4):SL1–SL20

Kley J, Franzke HJ, Jähne F, Krawczyk C, Lohr T, Reicherter K, Scheck-Wenderoth M, Sippel J, Tanner D, van Gent H, the SPP Structural Geology Group (2008) Strain and stress. In: Littke R, Bayer U, Gajewski D, Nelskamp S (eds) Dynamics of complex intracontinental basins: the Central European Basin System, Springer, Berlin, pp 97–124

Kockel F (2002) Rifting processes in NW-Germany and the German North Sea sector. Neth J Geosci 81:149–158

Kockel F, Krull P (1995) Endlagerung stark wärmeentwickelnder radioaktiver Abfalle in tiefen geologischen Formationen Deutschlands: Untersuchung und Bewertung von Salzformationen. Bundesanstalt für Geowissenschaften und Rohstoffe

Kozur H, Bachmann G (2008) Updated correlation of the Germanic Triassic with the Tethyan scale and assigned numeric ages. In: Krystyn L, Mandl GW (eds) Upper Triassic subdivisions, zonations and events, vol 76, Ber d Geol Bundesanst, pp 53–58

Kukla PA, Urai JL, Mohr M (2008) Dynamics of salt structures. In: Littke R, Bayer U, Gajewski D, Nelskamp S (eds) Dynamics of complex intracontinental basins: the Central European Basin System. Springer, Berlin, pp 291–306

Lepper J, Röhling H, der DSK SPT (2013) Stratigraphie von Deutschland XI: Buntsandstein. No. Bd. 11 in Schriftenreihe der Deutschen Gesellschaft für Geowissenschaften, Schweizerbart'sche, E

Leveille JP, Jones IF, Zhou ZZ, Wang B, Liu F (2011) Subsalt imaging for exploration, production, and development: a review. Geophysics 76(5):WB3–WB20

Littke R, Scheck-Wenderoth M, Brix MR, Nelskamp S (2008) Subsidence, inversion and evolution of the thermal field. In: Littke R, Bayer U, Gajewski D, Nelskamp S (eds) Dynamics of complex intracontinental basins: the Central European Basin System. Springer, Berlin, pp 125–153

Lohr T, Krawczyk C, Tanner D, Samiee R, Endres H, Oncken O, Trappe H, Kukla P (2007) Strain partitioning due to salt: insights from interpretation of a 3D seismic data set in the NW German basin. Basin Res 19(4):579–597

Maystrenko Y, Bayer U, Scheck-Wenderoth M (2005a) Structure and evolution of the Glueckstadt Graben due to salt movements. Int J Earth Sci 94(5–6):799–814

Maystrenko Y, Bayer U, Scheck-Wenderoth M (2005b) The Glueckstadt Graben, a sedimentary record between the North and Baltic Sea in north Central Europe. Tectonophysics 397(1):113–126

Maystrenko Y, Bayer U, Scheck-Wenderoth M (2006) 3D reconstruction of salt movements within the deepest post-Permian structure of the Central European Basin System-the Glueckstadt Graben. Neth J Geosci 85(3):181

Maystrenko YP, Bayer U, Scheck-Wenderoth M (2013) Salt as a 3D element in structural modeling—example from the Central European Basin System. Tectonophysics 591:62–82

Mohr M, Kukla P, Urai J, Bresser G (2005) Multiphase salt tectonic evolution in NW Germany: seismic interpretation and retro-deformation. Int J Earth Sci 94(5–6):917–940

Mohr M, Warren JK, Kukla PA, Urai JL, Irmen A (2007) Subsurface seismic record of salt glaciers in an extensional intracontinental setting (Late Triassic of northwestern Germany). Geology 35(11):963–966

Nalpas T, Brun JP (1993) Salt flow and diapirism related to extension at crustal scale. Tectonophysics 228(3):349–362

Peel FJ (2014) How do salt withdrawal minibasins form? Insights from forward modelling, and implications for hydrocarbon migration. Tectonophysics 630:222–235

Purvis K, Okkerman JA (1996) Inversion of reservoir quality by early diagenesis: an example from the Triassic Buntsandstein, offshore the Netherlands. In: Geology of gas and oil under the Netherlands. Springer, pp 179–189

Quirk DG, Pilcher RS (2012) Flip–flop salt tectonics. Geol Soc Lond Spec Publ 363(1):245–264

Reinhold K, Krull P, Kockel F (2008) Salzstrukturen Norddeutschlands, Geologische Karte 1:500 000. Bundesanstalt für Geowissenschaften und Rohstoffe

Rodon S, Littke R (2005) Thermal maturity in the Central European Basin System (Schleswig-Holstein area): results of 1D basin modelling and new maturity maps. Int J Earth Sci 94(5–6):815–833

Röhling HG, Gast RE (1991) A lithostratigraphic subdivision of the Lower Triassic in the northwest German lowlands and the German sector of the North Sea, based on gamma-ray and sonic logs. The perennial Rotliegend saline lake in northwest Germany. Geologisches Jahrbuch A 119:3–24

Rowan MG (1993) A systematic technique for the sequential restoration of salt structures. Tectonophysics 228(3):331–348

Rowan MG, Ratliff RA (2012) Cross-section restoration of salt-related deformation: best practices and potential pitfalls. J Struct Geol 41:24–37

Sannemann D (1968) Salt-stock Families in Northwestern Germany. AAPG Mem. 8:261–270

Scheck-Wenderoth M, Lamarche J (2005) Crustal memory and basin evolution in the Central European Basin System—new insights from a 3D structural model. Tectonophysics 397(1):143–165

Scheck-Wenderoth M, Krzywiec P, Zühlke R, Maystrenko Y, Froitzheim N (2008a) Permian to Cretaceous tectonics. In: McCann T (ed) The geology of Central Europe. The Geological Society of London, pp 999–1030

Scheck-Wenderoth M, Maystrenko Y, Hbscher C, Hansen M, Mazur S (2008b) Dynamics of salt basin. In: Littke R, Bayer U, Gajewski

D, Nelskamp S (eds) Dynamics of complex intracontinental basins: the Central European Basin System. Springer, Berlin, pp 307–321

Schöner R (2006) Comparison of Rotliegend sandstone diagenesis from the northern and southern margin of the North German Basin, and implications for the importance of organic maturation and migration. Dissertation, Univ. Jena

Sclater JG, Christie PAF (1980) Continental stretching: an explanation of the post-mid-Cretaceous subsidence of the Central North Sea basin. J Geophys Res Solid Earth (1978–2012) 85(B7):3711–3739

Seni SJ, Jackson MPA (1983) Evolution of salt structures, East Texas diapir province, part 1: sedimentary record of halokinesis. AAPG Bull 67(8):1219–1244

Sørensen K (1998) The salt pillow to diapir transition: evidence from unroofing unconformities in the Norwegian-Danish Basin. Pet Geosci 4(3):193–202

Stewart SA (2007) Salt tectonics in the North Sea Basin: a structural style template for seismic interpreters. Spec Publ Geol Soc Lond 272:361

Stollhofen H, Bachmann GH, Barnasch J, Bayer U, Beutler G, Franz M, Kästner M, Legler B, Mutterlose J, Radies D (2008) Upper Rotliegend to Early Cretaceous basin development. In: Littke R, Bayer U, Gajewski D, Nelskamp S (eds) Dynamics of complex intracontinental basins: the Central European Basin System. Springer, Berlin, pp 181–207

Trusheim F (1960) Mechanism of salt migration in northern Germany. AAPG Bull 44(9):1519–1540

Urai JL, Schléder Z, Spiers CJ, Kukla PA (2008) Flow and transport properties of salt rocks. In: Littke R, Bayer U, Gajewski D, Nelskamp S (eds) Dynamics of complex intracontinental basins: the Central European Basin System. Springer, Berlin, pp 277–290

Van Wees JD, Stephenson RA, Ziegler PA, Bayer U, McCann T, Dadlez R, Gaupp R, Narkiewicz M, Bitzer F, Scheck M (2000) On the origin of the southern Permian Basin, Central Europe. Mar Pet Geol 17(1):43–59

Warsitzka M, Kley J, Kukowski N (2013) Salt diapirism driven by differential loading—some insights from analogue modelling. Tectonophysics 591:83–97

Warsitzka M, Kley J, Kukowski N (2015) Analogue experiments of salt flow and pillow growth due to basement faulting and differential loading. Solid Earth 6(1):9–31

Wolfgramm M, Rauppach K, Seibt P (2008) Reservoir—geological characterization of Mesozoic sandstones in the North German Basin by petrophysical and petrographical data. Zeitschrift für geologische Wissenschaften 36:249–265

Yegorova T, Maystrenko Y, Bayer U, Scheck-Wenderoth M (2008) The Glueckstadt Graben of the North-German Basin: new insights into the structure from 3D and 2D gravity analyses. Int J Earth Sci 97(5):915–930

Yoon MK, Baykulov M, Dümmong S, Brink HJ, Gajewski D (2009) Reprocessing of deep seismic reflection data from the North German Basin with the common reflection surface stack. Tectonophysics 472(1):273–283

Ziegler PA (1982) Triassic rifts and facies patterns in Western and Central Europe. Geologische Rundschau 71(3):747–772

Ziegler PA (1990) Geological Atlas of Western and Central Europe, 1990. Geological Atlas of Western and Central Europe, Shell Internationale Petroleum Maatschappij, B.V

Zirngast M (1996) The development of the Gorleben salt dome (northwest Germany) based on quantitative analysis of peripheral sinks. Geol Soc Lond Spec Publ 100(1):203–226